FILM THICKNESS MONITOR FOR THE CONTROLLED

EVAPORATION OF VACUUM DEPOSITED FILMS

FILM THICKNESS MONITOR FOR THE CONTROLLED

EVAPORATION OF VACUUM DEPOSITED FILMS

By

LEONHARD GROTH, B. ENG.

A Thesis

Submitted to the Faculty of Graduate Studies

in Partial Fulfilment of the Requirements

for the Degree

Master of Engineering

McMaster University

May 1968

ABSTRACT

A thin film thickness monitor has been designed and
constructed based on the "mass loading" effect of a resonant
quartz crystal. A 6.0 MHz Y-cut crystal, having a theoretical
"mass determination sensitivity" of 8.15×10^7 Hz. $- cm^2/gm$,
serves as the sensor element. This sensitivity can be close-
ly approached in practice if the entire active area of the
quartz plate is exposed to the evaporant stream. However, due
to source, substrate and crystal geometry the "effective" sen-
sitivity of the monitor is only 0.433 of the above value.

Both film thickness and deposition rate can be mea-
sured by the monitor in terms of equivalent frequency changes.
The actual thickness and rates depend upon the density of the
evaporant. In the case of silver (density 10.5 gm/cm^3), the
monitor measures average thicknesses from several Å to 1.36
microns in one single deposition. Each crystal can be used
to monitor a total of 4.5 microns of silver before replacement.
Deposition rates for silver can be measured from as low as
0.1 Å/sec. to 1360 Å/sec.

By combining the thickness monitor with apparatus for
controlled evaporation, a system was set up which can control
film thickness to within 2% and deposition rate to within 5%.

(iii)

MASTER OF ENGINEERING (1968)   McMASTER UNIVERSITY
(Electrical Engineering)   Hamilton, Ontario.

TITLE: Film Thickness Monitor for the Controlled
         Evaporation of Vacuum Deposited Films

AUTHOR: Leonhard Groth, B. Eng. (McMaster University)

SUPERVISOR: Professor C. K. Campbell

NUMBER OF PAGES: ix, 96

SCOPE OF CONTENTS:

In this thesis the theory, design and performance
of an instrument using a resonating quartz crystal to mea-
sure the thickness and deposition rate of in vacuo deposited
films is described. The relationship between the change in
frequency of the quartz crystal and the deposited film thick-
ness is derived. The sensitivity of the crystal, as well as
the effect of the source evaporation characteristic and the
source, substrate and crystal geometry are investigated. The
design of the electronic circuitry of the instrument is des-
cribed in some detail. The integration of this instrument
with appropriate control equipment to set up a system for
controlled rate and thickness is then described and the per-
formance of this system experimentally evaluated.

ACKNOWLEDGMENTS

TABLE OF CONTENTS   PAGE

LIST OF FIGURES   PAGE

LIST OF FIGURES   PAGE

CHAPTER 1

1.1 Introduction

It has been well established that the formation and structure of in vacuum deposited thin films are very much dependent on the deposition parameters. Since the formation and resulting structure of the films determine to a large extent the physical properties they will possess, these properties will then largely be determined by the same deposition parameters. It is therefore important that as many of these parameters as possible be under close control during the deposition if vacuum deposited thin films are to be made reproducible in every respect.

The important parameters which largely determine the formation and structure of a thin film and hence its properties are as follows:

--nature and partial pressure of the residual gases
  of the atmosphere in which films are deposited
--surface conditions and nature of substrate
--substrate temperature
--rate of deposition and hence rate of evaporation
--final film thickness.

All the above parameters, with the exception of rate of deposition and film thickness, are independent of the process of laying down the film and can be selected or adjusted

1

as desired prior to evaporation. However, the best control over the rate of deposition and final film thickness is obtained by monitoring these parameters during deposition. Consequently, a system which permits a simultaneous measurement of rate of deposition and thickness is a necessity if thin films with reproducible characteristics are to be made.

The effect of the deposition parameters on the growth and structure of thin films has been well investigated and described.[1,2] In particular, the rate of deposition of material on the substrate and the substrate temperature combine to have a pronounced effect on thin film structure.

At low deposition rates, initial film formation or nucleation is low, and condensed mobile atoms have a long mean free time before reaching a lattice site. This results in large diameter crystallites with definite preference for those crystallographic orientations representing the lowest free energy. The film appears rough and granular. Increased deposition rates result in a decrease in average crystallite size until at high rates mobile condensed atoms become buried before reaching appropriate lattice sites resulting in completely amorphous but smooth films.

Substrate temperature is important since it affects the surface mobility of condensed atoms. In general the size of the crystallites increases and the number of defects decreases as the surface mobility of condensed atoms increases

with temperature.

Knowledge of the thickness of a film is desire-
able since the resistance of a given film, for example, is
dependent on the cross-sectional area. Additional affects
in resistance occurs when the film thickness becomes com-
parable with the mean free path of the conduction electrons.
Furthermore, very thin films consist of small isolated is-
lands of condensed material and consequently may be elec-
trically discontinuous.

From a practical viewpoint, knowledge of film thick-
ness is essential in the production of thin film resistors
and capacitors for micro-electronic circuits where compo-
nent values are determined by physical size and by sheet
resistivity and dielectric thickness respectively.

1.2 Methods of Measuring Thin Film Rate and Thickness

Since the rate of deposition and final film thick-
ness are desirable properties to know about a deposited
film, a number of methods for measuring them have been
devised.

Optical methods of measuring thin film thickness
are among the most common. Either a multiple beam inter-
ferometer can be used for direct measurement,[3] or thickness
can be obtained from measurements of the reflectance or
transmittance properties of the film using a modulated
light beam photometer.[4] The latter are especially useful

for producing thin film optical filters.

Mechanical methods for measuring film thickness include the use of some form of microbalance used either inside or outside the vacuum apparatus. Average thickness of the film is calculated by dividing the total mass of the film by area of deposition and density. Corrections, however, have to be made for differences between thin film and bulk density.

Methods that measure the rate of deposition provide an advantage, since in addition to rate, film thickness can be obtained by a suitable integration technique. Mechanically a measure of deposition rate can be obtained by measuring the impact on a light metal vane exposed to a portion of the evaporant stream.[5] Rate of evaporant flow and hence deposition can also be measured by ionizing a portion of the evaporant vapour stream. The resulting ion current is a measure of the evaporation rate.[6,7]

A completely different method of measuring film thickness and rate deposition is achieved by using a resonating quartz crystal vibrating in a particular mode.[8,9] When the vibrating surface of the quartz crystal is exposed to the vapour stream, and the material allowed to condense the frequency of resonance decreases linearly with the amount of mass deposited on the crystal surface. The rate of change of frequency (Hz./sec.) provides a measure of the rate of deposition. The total change in frequency (Hz.) provides

a measure of the mass deposited from which film thickness can be obtained.

Since the quartz crystal method measures deposited mass, perhaps a more appropriate measure of the deposited film would be its surface density (gm./cm.^{2}). Indeed this is a more meaningful term when very thin films, consisting of isolating islands are deposited. However, the change in resonant frequency can also be calibrated in terms of thickness (angstroms) by comparison with thickness measurements made on the film, for example, by a multiple-beam interferometer.

The quartz crystal "mass loading technique" of measuring deposition rate and film thickness, although less direct than some of the other methods indicated above, has a number of definite advantages. Firstly, it combines high sensitivity with operational simplicity as compared to, say, in vacuo microbalances. Secondly, it provides signals of both film thickness and deposition rate and hence can be used for the automatic control of these parameters. Finally, it has also found application in other areas of study as, for example, in studies of surface contamination in vacuum systems or gas sorption by evaporated films.[10,11]

1.3 Scope of Thesis

The purpose of this thesis is to describe the development of a thin film thickness and deposition rate monitor based on the mass loading effect of a resonating quartz crystal. This monitor is to be used to prepare controlled rate and thickness deposited thin films made in vacuo using resistance heated sources.

Since the quartz crystal is the heart of the monitor the parameters which determine the sensitivity and accuracy of this sensor are discussed. The relationship and linearity between deposited mass and resultant frequency change are presented. In addition the effect of the type of evaporant source, as well as the geometry of source, substrate and crystal positions are also discussed.

The complete electronic system for measuring the change and rate of change of frequency was designed and constructed. Aspects of this design and the electronic circuitry are discussed in some detail.

To get meaningful results, the completed monitor was first calibrated to provide accurate measurements of change and rate of change of the resonant frequency of the quartz crystal. A series of depositions with silver were then made to calibrate these frequency measurements in terms of Angstrom and Angstrom/sec. respectively.

Finally the monitor was integrated with appropriate control circuitry to complete a system for controlled rate

and thickness deposition. Some examples of controlled
depositions obtained with this system are shown and dis-
cussed.

CHAPTER 2

Theory of Quartz Crystal Sensor

2.1 Introduction

The heart of the thin film rate and thickness
monitor to be described is the resonating quartz crystal
sensor. Since the frequency change of the sensor due to
mass loading is largely determined by the properties of the
crystal, some understanding of these properties is required
to obtain optimum performance. The purpose of this chapter
then is to discuss the basic operation of the quartz crystal
sensor, as well as the sensitivity of this operation to the
parameters of the quartz crystal and the ambient conditions.

2.2 Some properties of Crystalline Quartz Plates

The material from which the resonating crystal is
cut is crystalline silicon dioxide. The idealized appearance
of such a quartz crystal is shown in Figure 2.1 below. In
this figure, the z or optical axis is an axis of threefold
symmetry i.e. any property measured at a particular point has
the same value at a point $\pm$ 120 degrees about the z axis.
Furthermore, quartz has an anisotropic structure; therefore,
its physical properties are functions of the direction in

8

which these properties are considered.

The most important characteristic of quartz, however, is its piezoelectric property. Because of this property, an electric field applied perpendicular to a plate of quartz causes it to undergo mechanical deformation. The deformation in turn gives rise to an electric potential. In this manner the quartz plate can be made to vibrate mechanically at a frequency which is a function of the physical properties of the quartz as well as the geometrical dimensions.

Depending on the shape of the quartz plate, kind of cut, and manner of excitation, a number of modes of vibration are possible.[12] The vibrational mode of crystals used as mass or thickness sensors employ the thickness shear mode of oscillation. This is shown diagramatically in Figure 2.2. In this mode of oscillation the crystal faces slide in parallel but opposite directions, forming a node in the centre plane and antinodes on the surface. To prevent the presence of unwanted modes of vibration the crystal plates are cut to specific dimensions. Dimensional ratios can be obtained for which only the main mode exists for a large frequency range on either side of the main frequency.[13]

The angles of cut of particular interest in the present application are the special Y-cuts which make various angles with respect to the z axis as shown in Figure 2.3. The various cuts aim at obtaining desired properties for the
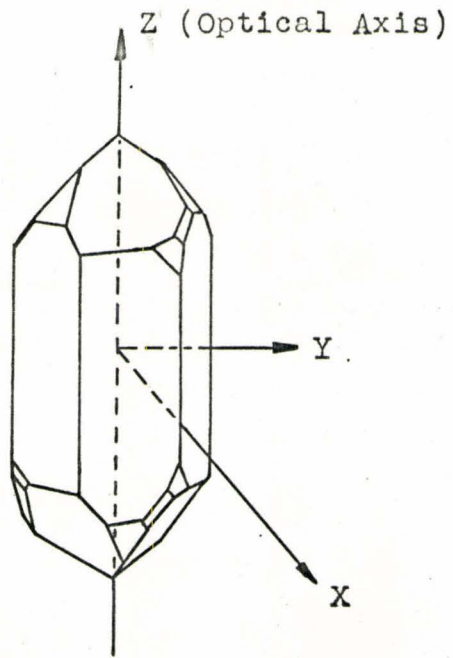
Figure 2.1

Idealized Appearance of Natural Quartz Crystal.
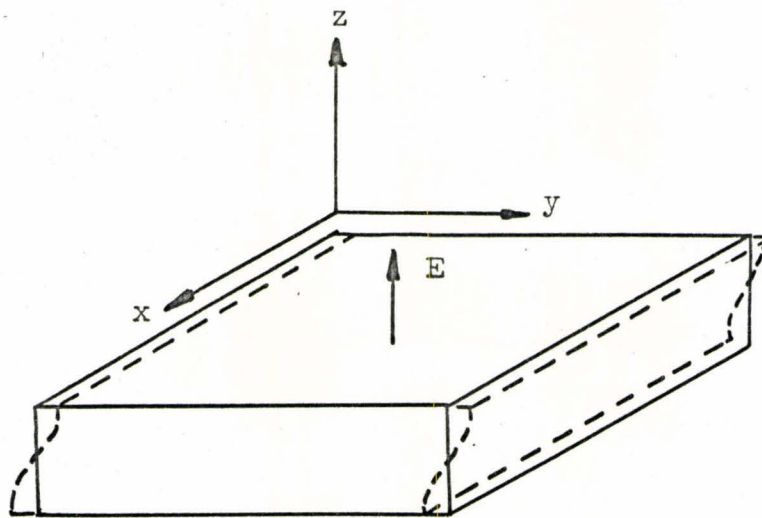
Figure 2.2

Shear Thickness Mode of Oscillation of Quartz Crystal.

resonating crystals. A zero temperature coefficient of frequency and thickness shear mode of oscillation are the present requirements. The AT cut with an angle of $35^{\circ}15'$ with respect to the z axis and the BT cut of angle -49° degrees have these properties.

The effect of temperature for AT and BT cuts is shown by the curves in Figure 2.4. AT cut curves follow a generally cubic law while BT cuts follow a generally parabolic law. Since the AT cut has a zero temperature coefficient of frequency over the range -5 to +55 degrees centigrade, it is the most frequently used crystal cut for mass or thickness monitoring purposes.

2.3 Natural Frequency of Resonance of Quartz Plate

For a quartz crystal of either AT or BT cut resonating in a thickness shear mode the frequency of resonance is given by[12]

$$f = \frac{n}{2d} \sqrt{\frac{c}{p_q}}$$
<div align="right">Eqn. 2.1</div>

where n is the harmonic order, d the thickness of quartz plate, c the shear elastic stiffness constant, and p_q the density of quartz. Calling

$$\frac{1}{2} \sqrt{\frac{c}{p_q}} = N$$

then
$$f = \frac{N}{d}.$$
<div align="right">Eqn. 2.2</div>
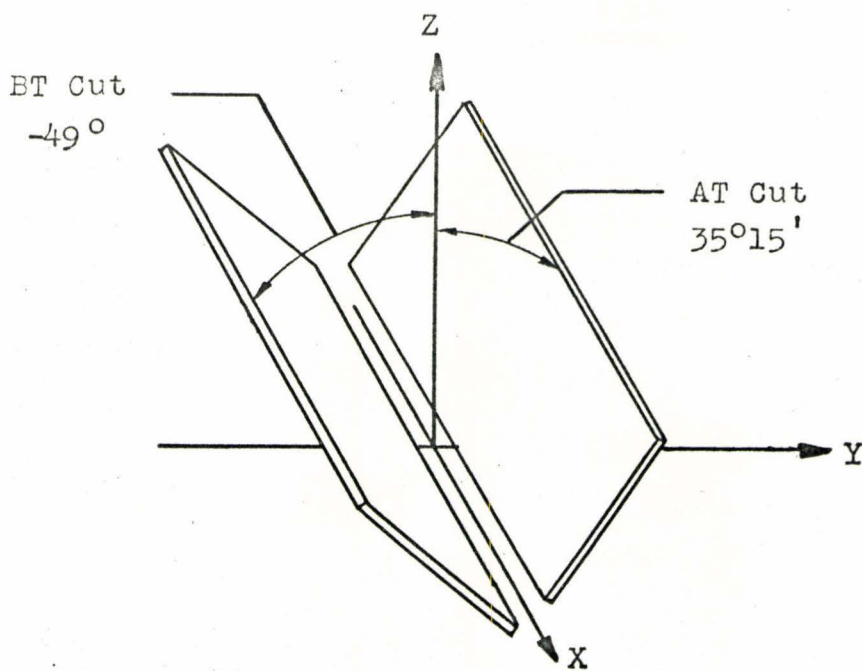
Figure 2.3

Y-cut quartz plates.
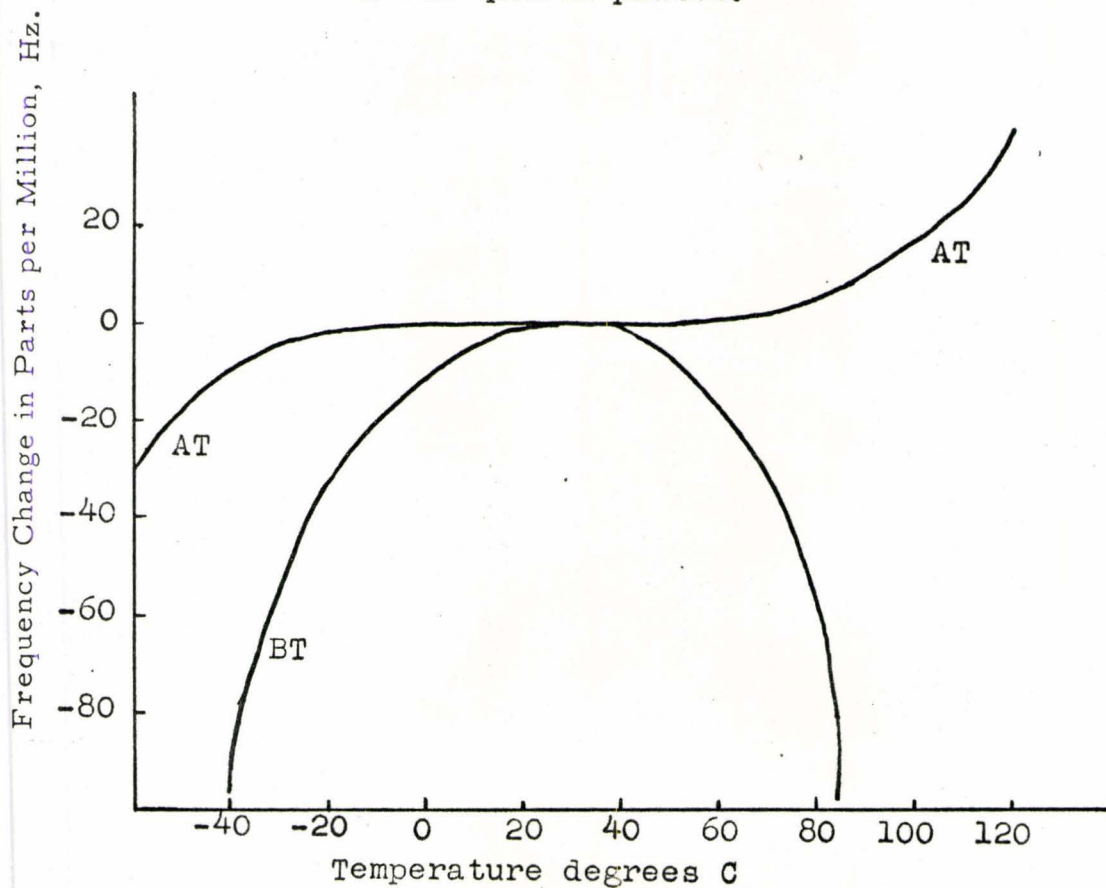
Figure 2.4   Temperature coefficient of frequency of Y-cut
quartz crystals.

For an AT cut crystal N=1670 KHz/mm, whereas for a BT cut crystal N=2500 KHz/mm.

2.4 Theory of Mass Loading of Resonant Crystal

As shown in Figure 2.2, a quartz plate oscillating in the thickness shear mode forms antinodes at its surfaces. It has been found by Sauerbrey[8] that when a small amount of mass is deposited on either of these antinodal surfaces the frequency of vibration of the crystal is decreased. Since the material is deposited on the antinodal surfaces, it will effect the frequency insofar as it has inertial mass. Provided the amount of mass added is small compared to the mass of the crystal the resultant change in frequency is independent of the elastic constant of the added material.

The relationship between decrease in frequency of the resonating crystal and added mass can best be derived by using perturbation analysis.[14]

If the inertia or the elastic stiffness of a mechanically vibrating system are changed by a small amount, the resonant frequency $f_{o,n}$ is perturbed according to

$$f_n^2 = f_{o,n}^2 \frac{(1 + \Delta C_{nn}/C_n)}{(1 + \Delta a_{nn}/a_n)} \qquad \text{Eqn. 2.3}$$

where f_n is the perturbed frequency, $f_{o,n}$ is the unperturbed frequency, and C and a are coefficients in quadratic expansion for the potential and kinetic energies of the system.[15]

If the added mass is small compared to the total mass of the crystal and if it is added to an antinode of vibration, then we can assume it stores kinetic energy only. Hence the potential term $\Delta C_{nn} = 0$. Substituting in equation 2.3, then

$$f_n^2 = f_o^2, n \frac{1}{(1 + \frac{\Delta a_{nn}}{a_n})}. \qquad \text{Eqn. 2.4}$$

When adding perturbing mass to a resonant plate the co-efficients in equation 2.4 becomes

$$a_n = \frac{p_q}{2} \int_V U^2 \, dV, \qquad \Delta a_{nn} = \frac{1}{2} \int_A \sigma (U (\frac{d}{2})^2) \, dA$$

where σ is the mass added per unit area, d the thickness of vibrating quartz plate, U the velocity of plate at any point, V the volume of plate in motion, A the area of plate in motion, and p_q the density of the quartz.

The above integrals cannot be evaluated, for the following reasons:

-- the perturbing mass may not be added uniformly over the antinodal surface

-- area over which mass is added may not coincide with A, the active area of the crystal

-- the variation of displacement throughout the volume of the crystal is not known.

To account for the above portions of the integrals that

cannot be performed three constants k_1, k_2, k_3 are introduced.
Thus Equation 2.4 becomes

$$f_n^2 = f_{n,o}^2 \; \frac{1}{1 - \dfrac{k_1 m}{A} \dfrac{k_2 k_3 2}{p_q d}} \; , \qquad \text{Eqn. 2.5}$$

where m is the total mass added to the crystal. If the crystal
is to operate in the fundamental mode n=o and hence the change
in frequency is

$$\Delta f = (f - f_o) \simeq - \frac{f_o K m}{d p_q A} . \qquad \text{Eqn. 2.6}$$

Since in equation 2.6 $k_1, k_2,$ and k_3 are not individually known
they have been replaced by one constant K. Substituting
equation 2.2 for d in the above equation the final result
is obtained, namely

$$\Delta f = \frac{- f_o^2 K}{N p_q} \frac{m}{A} . \qquad \text{Eqn. 2.7}$$

Equation 2.7 indicates the relationship between the
decrease in frequency and the mass added to the crystal sur-
face. The term $\dfrac{f_o^2 K}{p_q N}$ is known as the "mass determination sen-
sitivity" in the literature.[8] The aggregate factor K is
unity or near unity when the added mass is distributed uni-
formly over the entire active area of the crystal.[8,14]
With K taken as unity the factor $C_f = \dfrac{f_o^2}{p_q N}$ is defined
as the theoretical sensitivity. It can be calculated from

the crystal parameters since f_o, p_q and N are known. Now
from equation 2.8 C_f is proportional to the square of the
resonating frequency. Hence quartz crystals with higher re-
sonant frequencies can measure smaller amounts of mass. To
illustrate this a number of values of C_f for AT-cut crystals
of different f_o are shown in the table below. (The density
of quartz is taken to be 2.65 g/cm^3.)

TABLE 1

Mass Determination Sensitivity for various Resonant Frequencies

f_o, MHz	C_f, Hz-cm^2/gm	Δm, gm/cm^2	Δt, $\overset{o}{A}$, Δf=1 Hz)
1	2.26 x 10^6	4.42 x 10^{-7}	4.42
6	8.15 x 10^7	1.23 x 10^{-8}	1.23
10	2.26 x 10^8	4.42 x 10^{-9}	0.442

In the present application of the quartz crystal sen-
sor the desired parameter to be measured is film thickness.
This can be obtained from Equation 2.7 by using the relation-
ship $\frac{m}{A} = p_m t$ where m is the added mass, A the area of deposi-
tion, p_m the density of the material and the average film
thickness. Then

$$t = \frac{N p_q |\Delta f|}{f_o^2 K p_m} = \frac{|\Delta f|}{C_f p_m}$$

Eqn. 2.8

Column 4 in Table 1 gives the equivalent thickness in Ang-
stroms of a deposited film for a change of frequency of 1 Hz
and a unity density material for several values of f_o.

2.5 Linearity Between Mass and Frequency Change

The relationship between mass deposited on the quartz crystal and change in resonant frequency of the crystal is not linear. This is due to the fact that the mass determination sensitivity of C_f is proportional to f_o^2. Now with continued deposition on the crystal, its resonant frequency decreases and hence C_f decreases. Therefore, for equal increments in resonant frequency, increasing increments of mass must be added. When measuring film thickness, films of increasing thickness are obtained for equal and consecutive increments of frequency change.

It may be desirable to know the error in a film thickness due to this non-linearity. However, a more useful result is to calculate the total change in resonant frequency permissible for a certain specified error in film thickness, say 1%. In order to find this permissible change in frequency C_f in Equation 2.8 is allowed to become a variable, and integration with respect to f carried out. If the initial and final frequencies are f_1 and f_2 then the corresponding film thickness is

$$t_r = \frac{K' \Delta' f}{f_2 \, f_1}, \text{ where } \Delta' f = f_1 - f_2, \; K' = \frac{N p_q}{K p_m}. \quad \text{Eqn. 2.9}$$

The ideal thickness predicted by Equation 2.8 is

$$t_I = \frac{K' \Delta' f}{f_o^2}.$$

The fractional error between t_r and t_I is given by

$$\epsilon = \frac{t_r - t_I}{t_I} \qquad \text{Eqn. 2.10}$$

Since both $\Delta f = f_0 - f_2$ and $\Delta' f = f_1 - f_2$ are small compared to f_0, then

$$\epsilon = \frac{(2-k)\,\Delta f}{f_0} \qquad \text{Eqn. 2.11}$$

In Equation 2.11 $k = \dfrac{\Delta' f}{\Delta f}$ and has the range $0 < k \leq 1$ since the change in frequency $\Delta' f$ due to a deposition cannot be greater than the total in resonant frequency.

Rewriting Equation 2.11 the permissible change in resonant frequency of the quartz crystal from f_0 for a specified error is given by

$$\Delta f = \frac{\epsilon\, f_0}{(2-k)} \qquad \text{Eqn. 2.12}$$

Equation 2.12 states that for a 1% deviation in film thickness and $k \ll 1$ the permissible value of Δf is 1/2% of f_0. If $k \simeq 1$ then the permissible Δf if 1% of f_0. Table 2 below shows the permissible change in resonant frequency for a 1% deviation of film thickness and $k \ll 1$ for a number of frequencies.

TABLE 2

Permissible Frequency and Thickness Changes for a 1% Error

f_0 Hz.	f_p Hz.	gm/cm^2	t_p Å
1.0×10^6	5.0×10^3	2.23×10^{-3}	2.23×10^5
6.0×10^6	3.0×10^4	3.63×10^{-4}	3.63×10^4
1.0×10^7	5.0×10^4	2.23×10^{-4}	2.23×10^4

From Table 1 it is seen that the sensitivity of a crystal to film thickness increases as the square of the resonant frequency. However, Table 2 shows that the total permissible thickness (for a given error) that can be measured by the crystal decreases with frequency. Consequently, a compromise must be made between sensitivity and crystal life. This will depend largely on the application.

Of course, the crystal can be used beyond the permissible $\frac{1}{2}\%$ limit of f_o by sacrificing accuracy in film thickness. The other alternative is to calibrate the change in frequency of the crystal in terms of film thickness over the entire useful range.

Even if larger errors in measuring film thickness were tolerable or calibration is employed, the crystal can not be used indefinitely. There will come a point when the loading of the crystal will be sufficiently large to reduce the amplitude of oscillation beyond the measurable level or the oscillations may stop completely. When this occurs a new crystal is required or the deposit can be removed and the cleaned crystal used again.

2.6 Factors Affecting the Stability of the Resonant Frequency

During a deposition the frequency of the oscillating crystal can be affected by a number of other factors besides condensing matter. These changes in frequency result in an error in the frequency change due to added mass. Some of

the changes can be corrected for while others can not. The significance of this error is to introduce an error in the mass per area ratio or average film thickness measurement. Furthermore, they impose a limit on the accuracy with which the change in frequency can be measured by the associated electronic circuitry. Some of these sources of crystal frequency instability are due to the physical properties of the quartz crystal, while others are due to the electronic measuring circuits.

One of the largest errors is due to temperature changes of the quartz crystal during deposition since the frequency is temperature dependent as indicated in section 2.2 above. Fortunately, this effect can be reduced by choosing a crystal cut having the smallest temperature coefficient of frequency (TCF) over the range of temperature which the crystal is likely to experience. As indicated in the above section, the best crystal cut for measuring thin film thickness is the AT cut with angle of 35° 15' since it has a zero TCF over the range -5° to 55°C.

Since the crystal must be exposed to a hot evaporant beam in order to measure mass, some heating is unavoidable. The amount of radiant heating from the source can be reduced however, by appropriate heat shielding to permit only a wide enough beam sufficient for measuring purposes. If, however, very small frequency changes are to be measured accurately, then a water or oil cooled crystal holder can be employed.[9,16]

Alternatively, by monitoring the change in temperature of the crystal corrections due to heating can be made.

A frequency transient also occurs when the crystal is subjected to sudden temperature changes.[9] The transient is caused by a relaxation of an interfacial stress between the vapour plated electrodes and the quartz surface.[17] One method of reducing this transient is to use parallel field excitation.[18] There is however, no permanent change in frequency due to this effect after cooling the crystal to its original temperature.

The crystal mounting can also affect the resonant frequency insofar as the leads attached to the electrodes can take part in the vibration. However, crystals oscillating in the thickness shear mode are designed to have little or no vibration at the edges. Hence edge mounting has little effect on either crystal activity or frequency.

Variations in gas pressure also affect crystal frequency. Typically the largest change occurs during evacuation of the vacuum chamber. During evaporation at high vacuum (10^{-6} torr) pressure variations of several orders have negligible effect on frequency and can therefore be neglected.[17]

It is also possible that the more the resonant frequency due to deposited matter on the crystal deviates from its original frequency, oscillations in other than the shear mode may become possible or even preferable.

When this occurs the frequency may jump appreciably or oscillations may cease completely. The crystal may oscillate again however when the thickness shear mode again becomes the preferable mode.[19]

The frequency of the crystal is also affected by parameter changes in the oscillator circuit as well as the amplitude of the oscillator drive level.[9] Below 5 M.Hz. instability due to amplitude is negligible compared to phase changes. Phase instability arises from variations in any component in the oscillator feedback loop. One possible source is the parallel capacitance of the crystal holder and conductor leads which shunt the crystal.

2.7 Importance of Source, Substrate and Crystal Geometry on Thickness Measurements

When the substrate upon which the thin film is to be deposited is not the same distance from the source as the monitoring crystal, then the thickness deposited on the substrate is not the same as the thickness on the crystal. This difference is also affected by the type of evaporant source, since the source determines the spatial distribution of the evaporating atoms or molecules. Both of these factors must be taken into account to relate the thickness, as measured by the crystal, to the actual film thickness on the substrate.

One of the most common sources used in vacuum evaporations is the dimpled foil boat. Evaporation from this

source occurs from the small dimple on the upper side of the foil. It has been shown by Knudsen[20] that for this source, the amount of mass evaporated in a certain directtion per second is a function of the cosine of the emission angle $\emptyset$. $\emptyset$ is the angle between the direction under consideration and the normal to the source surface as shown in Figure 2.5.

Suppose m grams of a material have been evaporated from a surface source. Following the cosine law, the amount of material dm evaporated from this source through a solid angle $d\omega$ is

$$dm = \frac{m}{\pi} \cos\emptyset \, d\omega \qquad \text{Eqn. 2.13}$$

The monitoring crystal is located at a distance r cm. from the source and inclined at an angle θ to the incident vapour stream. If the area of condensation for the crystal is dS_X, then the solid angle subtended by this area is

$$d\omega = \frac{\cos\theta}{r^2} \, dS_X \qquad \text{Eqn. 2.14}$$

The amount of material deposited on the crystal is therefore

$$dm = \frac{m}{\pi} \cos\emptyset \frac{\cos\theta}{r^2} \, dS_X \qquad \text{Eqn. 2.15}$$

If the density of the deposited material is p gm /cm^2 then $dm = p \, dS_X t_X$, where t_X is the average thickness of the film on the crystal. Substituting for dm in Equation 2.15
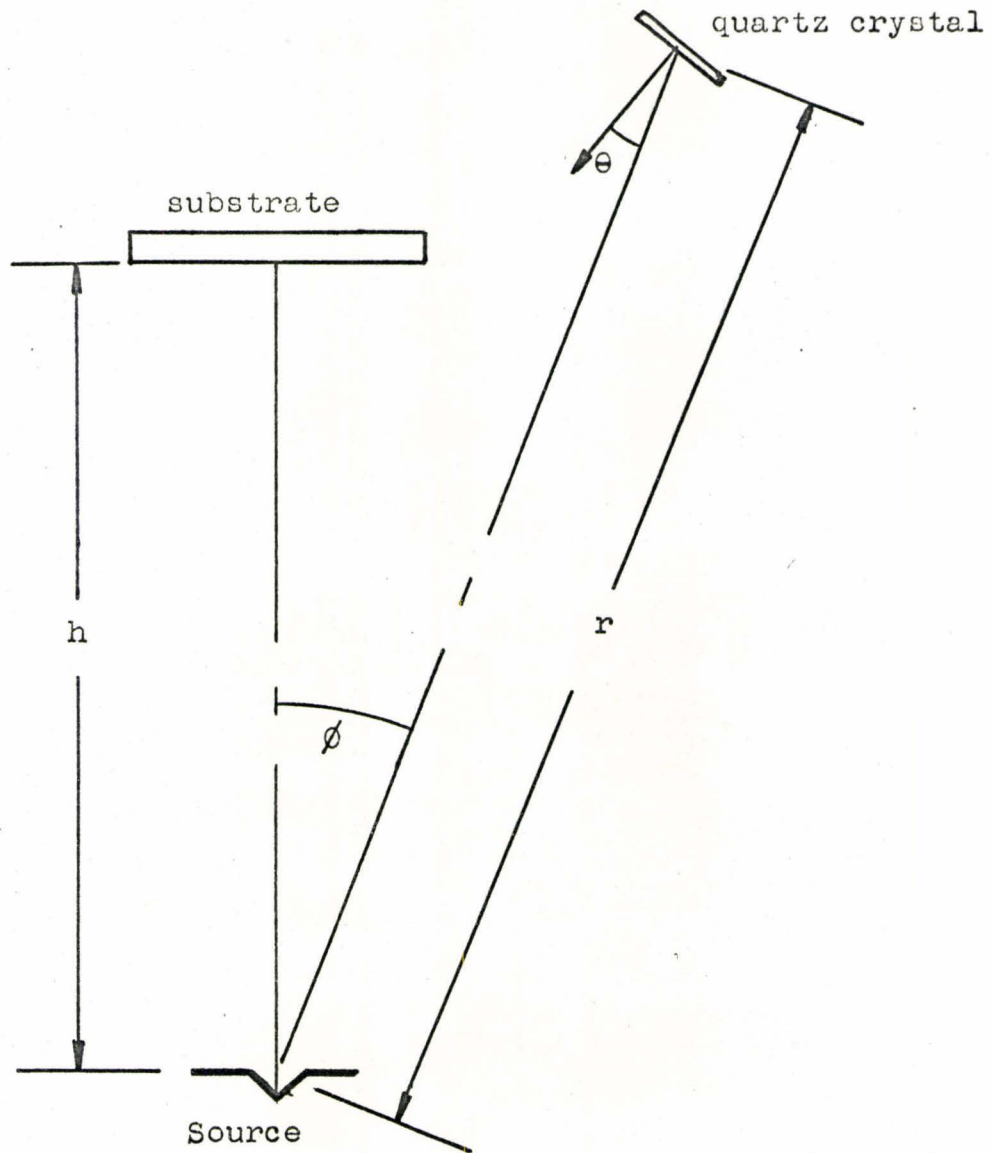
Figure 2.5

Source, substrate and crystal geometry

then

$$t_x = \frac{m}{\pi p} \frac{\cos \phi \cos \theta}{r^2} \qquad \text{Eqn. 2.16}$$

By similar argument the thickness of a film on a substrate h cm directly above and parallel to the source is

$$t_s = \frac{m}{\pi p} \frac{1}{h^2} \qquad \text{Eqn. 2.17}$$

Consequently, the relationship between measured thickness and substrate film thickness is

$$\frac{t_s}{t_x} = \frac{r^2}{h^2 \cos \phi \cos \theta} \qquad \text{Eqn. 2.18}$$

Equation 2.18 holds true only for a directed surface source. For a point source, radiating uniformly in all directions $\cos \phi$ and $\cos \theta$ are both zero and Equation 2.18 reduces to

$$\frac{t_s}{t_x} = \frac{r^2}{h^2} \qquad \text{Eqn. 2.19}$$

For tungsten conical basket sources or emission through apertures, the spatial distribution of evaporated atoms is best found empirically.[21]

2.8 Uniformity of Film Thickness over Substrate Surface

The thickness of a film evaporated on a plane parallel substrate from a simple source, such as a dimpled foil, is not uniform. This is due to the combined effect of spatial distribution of atoms being some function of the emission angle and the angle between the substrate

normal and the evaporant stream.

For the dimpled foil source for which Knudsen's cosine law holds, it can be shown that t_s, the thickness of the film anywhere on the substrate, is related to t_{so}, the thickness of the film at a point directly above the source, by

$$\frac{t_s}{t_{so}} = \frac{1}{[1 + (s/h)^2]^2} \qquad \text{Eqn. 2.20}$$

In this equation h is the source to substrate distance and s, the horizontal distance from any point on the substrate to the centre point of the substrate located directly above the source.

Equation 2.20 indicates that lines of constant film thickness are concentric circles centred on the substrate centre. Also film thickness decreases from the centre of the substrate to the periphery. In order to get nearly uniform thin films over the entire substrate surface, the ratio s/h must be made small compared to unity. If s/h cannot be made sufficiently small, then more elaborate sources must be employed.[22]

CHAPTER 3

Design, Description, and Construction of Thin Film Monitoring
Apparatus and Control System.

3.1 Introduction

In the last chapter the basic characteristics of a
quartz crystal thickness to frequency transducer were dis-
cussed. However, in order to take full advantage of these
features, instrumentation to measure the change and rate of
change of frequency easily and accurately is required. In
this chapter one approach to this problem is outlined. A
general outline of the proposed thickness monitor is first
given and then the circuitry discussed in detail. The
construction of a prototype instrument is described. This
instrument provides the signals for a complete controlled
thin film deposition system.

3.2 Design Objectives for Thickness Monitor

The thickness and rate monitor is to be used for
general deposition studies of thin film electronic devices.
This application requires an instrument which gives good
accuracy in the thickness measurements without demanding
stringent operating conditions or great skill on the part

of the operator. An instrument designed around a quartz crystal sensor fulfills these requirements well. In addition, it is sensitive only to the mass of the evaporated material; therefore, the deposition of a wide variety of materials can be monitored.

The selection of the fundamental resonant frequency of the quartz crystal involves a compromise between two desirable features. In practice, it would be advantageous to combine high crystal sensitivity with longest possible crystal life. However, as shown in Table 1 page 16, sensitivity increases as the square of the resonant frequency, while on the other hand crystal life for a given percent error decreases linearly with increasing frequency. This is shown in Table 2 page 18. For the present application, a resonant frequency combining "medium" sensitivity with longest possible crystal lifetime seems the best compromise.

Although quartz crystals operating in the range from one to fourteen megahertz have been used for thin film measurement applications,[8] five to six megahertz provides a better compromise between sensitivity and useful crystal life.[23] Since six megahertz AT-cut crystals were readily available from a local supplier, this frequency was therefore chosen. A six megahertz crystal has a thickness of 0.28 cm; therefore, it is also more easily handled during mounting and cleaning procedures.

The electronic circuitry of the thickness monitor must perform a number of functions. Most important, it must measure accurately the changes in crystal frequency due to deposition. Since these changes are relatively small, it is convenient to compare the monitor frequency with a reference frequency to obtain a more manageable intermediate frequency (I.F.). A stable variable oscillator can then be used to beat against the first I.F. to drive a counter circuit directly. The advantage of such a system is that when it is used with a multi-ranged pulse-analog counter, it can always be set back to its most sensitive range.[24] To obtain versatility the thickness monitor counter should have both meter and chart recorder readout facilities. In addition, it should also provide analog outputs for both thickness and rate depositon control. Finally while performing these functions the instrument should be rugged and reasonably simple to use.

3.3 Outline of Proposed Thickness Monitor

The outline of the proposed film thickness monitor based on the previous considerations is shown in block diagram form in figure 3.1. The monitoring crystal has an initial resonant frequency of six megahertz. The signal from this crystal is mixed with a reference frequency of 6.5 megahertz to provide a first I.F. of 0.5 megahertz having an increasing frequency with depositon characteristic.

Figure 3.1

Block Diagram of Rate and Thickness Monitor

This signal is mixed with a signal from the variable oscillator tunable over the anticipated range of the first I.F. frequency. This provides a second I.F. also having an increasing frequency with deposition characteristic. The variable oscillator is tuned to the first I.F. at the beginning of a typical deposition. Thus the second I.F. is initially zero and increases with deposition providing a signal proportional to the thickness of the deposit on the monitoring crystal.

After filtering and amplification, the second I.F. is applied to a Schmitt trigger, which squares up the waveform to provide sharp leading edges for the differentiating circuit that follows. The voltage spikes from the output of this circuit trigger a monostable multivibrator which provides constant area pulses for an integrating circuit. Analog readout is provided by a direct current milliammeter calibrated in hertz. By differentiating the analog thickness signal by a simple RC operational type differentiator, a signal proportional to the rate of change of frequency is obtained and measured by a microammeter. As indicated in the diagram DC voltages proportional to thickness and rate of deposition are available for controlled evaporation.

3.4 Details of the Quartz Crystal Sensor Head

The quartz crystal is the heart of the thickness

and rate monitor; it is mounted inside the vacuum coating chamber and exposed to a portion of the evaporant stream.

The shape of the actual crystal can be either square or round. The square crystals used were 12.7 mm to the side; the round ones have approximately a similar diameter. Gold electrodes are evaporated on both flat surfaces. Contact to these is made by spring clips which are soldered to two rigid mounting pins. These also serve as electrical conductors to support the crystal. These details are shown in Figure 3.2 below.
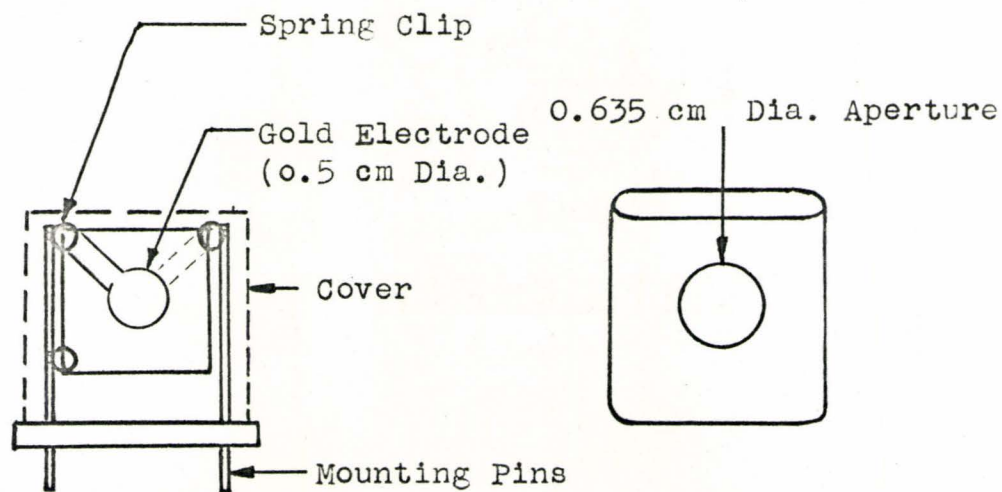
(a) Quartz Crystal Sensor   (b) Crystal Cover

Figure 3.2

Details of Quartz Crystal Mounting and Metal Cover.

A metal cover with a 0.25 inches (.635 cm) aperture is placed over the mounted crystal and spot soldered to the base. With the cover in position the 0.25 in. dia. hole is centered directly over the gold electrode. Since the aperture is slightly larger than the diameter of the gold electrode, the active area of the crystal is adequately covered. The use of the metal cover assures that always the same area of the crystal is covered during deposition. Critical crystal alignment now becomes unnecessary since the diameter of the evaporant stream impinging on the metal cover is larger than the 0.25 inches. The covered crystal is inserted into a holder which is surrounded by radiation shields for protection against excessive heating. The evaporant stream reaches the quartz crystals through a series of holes in this shielding. Consequently, total shielding is not possible. The shielding however, helps to assure that frequency changes of the crystal due to temperature are now small compared to changes due to deposited matter.

Connection between the crystal pins and the oscillator are made by heavy guage copper wire. As a result the resistance between crystal and oscillator is kept small. Also the rigidity of the wire prevents changes in the parallel capacitance across the crystal. Both of these factors help improve oscillator frequency stability.

3.5 Practical Design Considerations of the Oscillators

As shown in the block diagram Figure 3.1, the monitor employs three oscillators to obtain a signal frequency output with an increasing frequency with mass deposition characteristic. To design these oscillators, generalized two port network theory was employed.[25,26,27] From this analysis the condition for oscillations and the resonating frequency can be obtained. This analysis assumes linear operation even though self-sustained oscillation indicates nonlinear operation. Consequently, preliminary design calculations provide only approximate values and final design parameters are obtained by experimental adjustments.

The two important considerations in designing the three oscillators is to obtain adequate signal amplitude and good frequency stability. The latter is essential if the error in measuring the frequency change of the monitor crystal is to be kept to a minimum. The situation is aggravated by the fact that small differences between relatively large numbers are being measured. Since both the monitor and reference oscillators possess the stability associated with quartz crystals, the main source of frequency drift will be due to the variable oscillator. Therefore, extra steps need to be taken to assure the stability of this oscillator.

In any oscillator, changes in frequency are caused by changes in the parameters of either the active or the

passive devices. Changes in the former cause a change in the phase shift of the amplifier portion of the oscillator. In either case the feedback network has to provide an equal and opposite phase shift to keep the total phase shift of the oscillator loop equal to zero. This is achieved by a change in the frequency of the oscillator. Optimum frequency stability is obtained when the phase shift changes in the amplifier are a minimum and the phase shift of the feedback network with respect to frequency is a maximum.

A number of steps were taken to achieve frequency stability. The internal parameters of a transistor stage, for example, are dependent on its quiescent operating point, which in turn is a function of temperature and supply voltage. Therefore, the operating point must be held fixed by proper bias design and stabilized supply voltages. Transistor parameter changes due to load were minimized by the use of emitter follower buffer stages. The use of low input and output admittances in the feedback network reduces the influence of the input and output admittances of the transistor on frequency. Finally, circuit arrangements as, for example, the Clapp oscillator can be employed to achieve an improved stability characteristic.[28] The stability problem, most difficult to correct, arises from the changing of all parameters due to device aging. Since short term stability is the prime concern in this application, the effect of device aging on frequency stability can be completely neglected.

3.6 Detailed Discussion of Monitor Circuitry Oscillators
    and Intermediate Frequencies

The schematic diagram of the complete thin film
thickness and deposition rate monitor are given in Figures
3.3a and 3.3b. Throughout the following discussion frequent
reference will be made to these diagrams when discussing
devices or circuit functions. The values of the components
are specified in Appendix 1.

In Figure 3.3a both the monitor and reference oscil-
lators are basically transistorized Colpitts oscillators with
the quartz crystals providing the feedback. The crystals in
this circuit operate in the parallel resonant mode and are
electrically equivalent to an inductance. Design simplicity
is achieved by using untuned collector circuits for transis-
tors T_1 and T_8. This is desirable in the case of the monitor
oscillator since the frequency decreases with continued depo-
sition. Since the respective frequencies are close together,
the device values are essentially identical with the exception
of the feedback circuits. In the monitor oscillator capaci-
tors C_1 and C_2 are chosen to provide strong excitation to sus-
tain sufficient amplitude of oscillation during the useful
crystal lifetime. On the other hand C_{12} and C_{14} of the re-
ference oscillator are chosen to provide low distortion and
increased frequency stability.

Loading on both oscillator stages is reduced to a
minimum by emitter follower stages acting as buffers. In
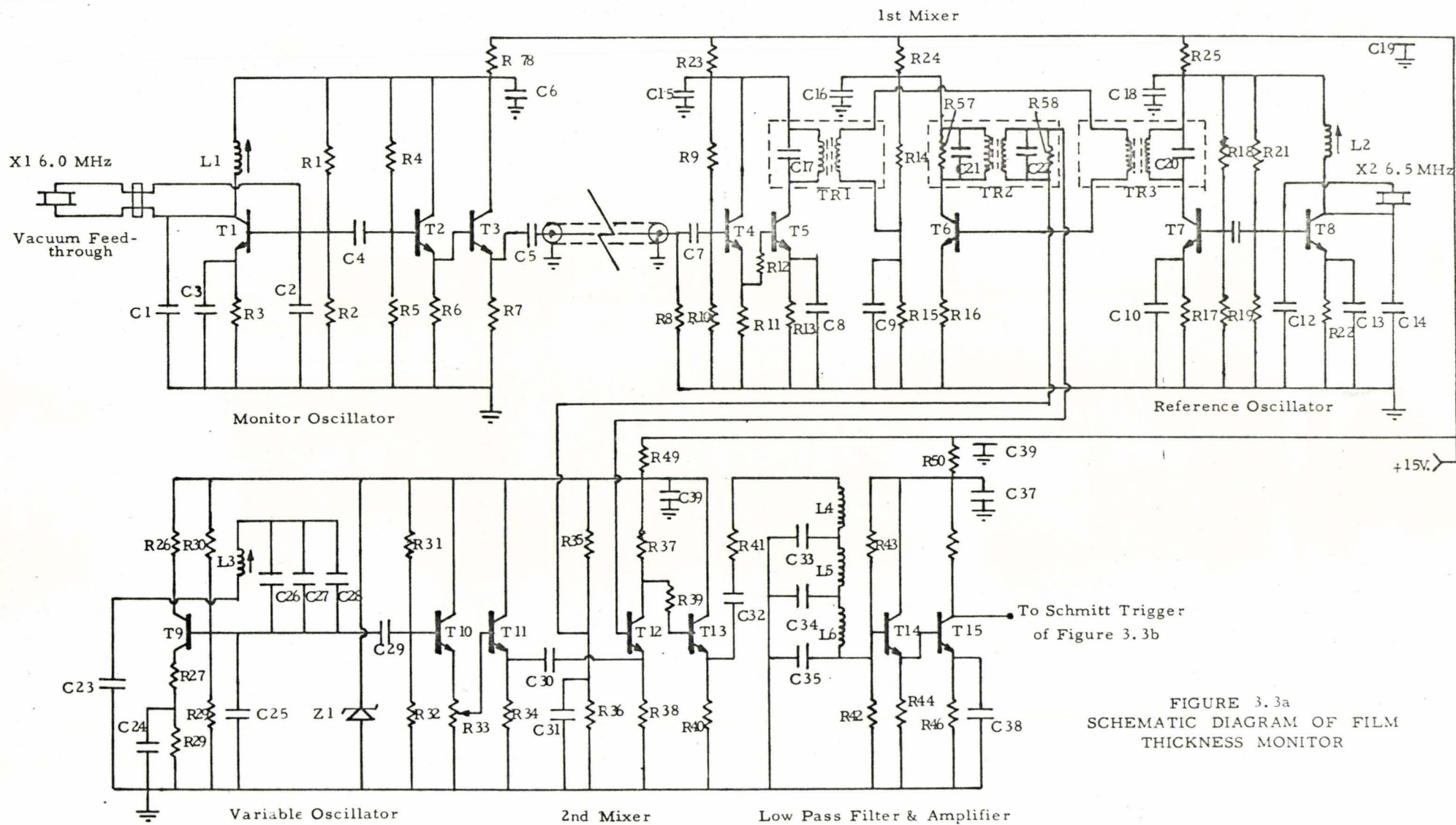
FIGURE 3.3a
SCHEMATIC DIAGRAM OF FILM
THICKNESS MONITOR
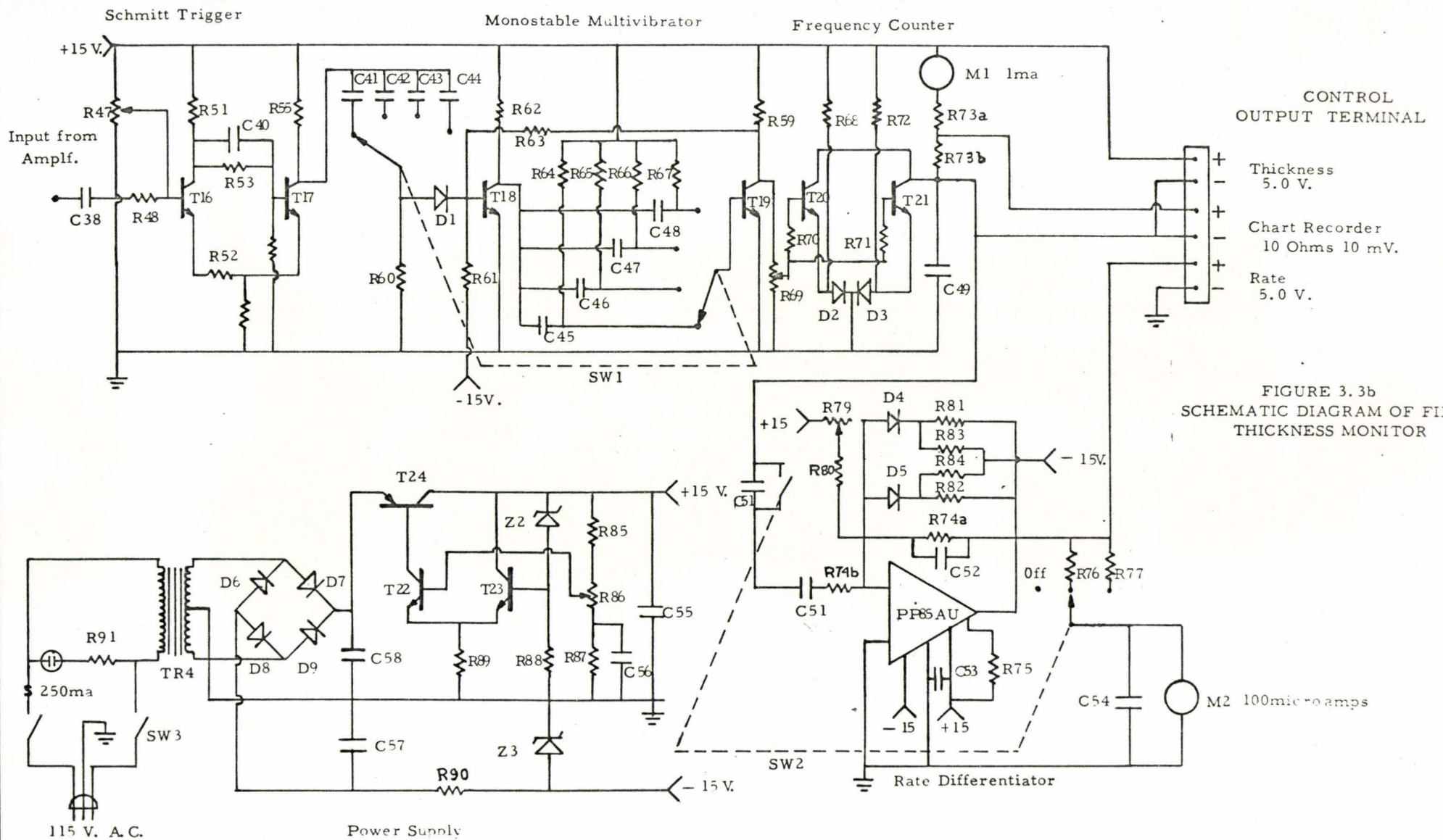
FIGURE 3.3b
SCHEMATIC DIAGRAM OF FILM
THICKNESS MONITOR

the monitor oscillator a second emitter follower stage, transistor T_3, is used to drive the 10 feet of 50 ohm coaxial cable, which transmits the signal to the main monitor unit. The cable is terminated by a matched resistive load to reduce signal distortion. The variable oscillator is required to provide a zero beat frequency for the first I.F. Consequently, it is tuneable over the range from 0.5 to 0.7 MHz. To achieve the desired frequency stability and tuning circuit simplicity, it was decided to employ a transistorized Clapp oscillator.[28] Referring to Figure 3.3a, inductance L_3 in series with the parallel combination of C_{26}, C_{27}, C_{28} determines the frequency of oscillation. C_{26} sets the upper frequency limit while C_{27} facilitates the main, and C_{28} the fine tuning. To enhance frequency stability C_{23} and C_{28} should be of the order of 0.002 to 0.005 microfarads.[29] In the present design C_{25} was reduced to the lower value of 330 picofarads since this gave a more uniform output over the tuning range. To enhance frequency stability, the supply voltage is stabilized by zener diode Z_1, and the loading buffered by transistor stages T_{10} and T_{11}.

Intermediate Frequencies

The monitor signal from the coaxial cable is amplified by transistors T_4 and T_5. The output from the latter together with the reference signal are coupled into the base of T_6 through single tuned transformers TR1 and TR3. T_6 is biased

in the non-linear region. A difference frequency can be extracted from this circuit because of the non-linearity between the emitter-collector current and the base-emitter voltage. In addition the circuit can provide gains of 20 to 25 db under optimum conditions.[30] The first I.F. is selected by the tuned output of transformer TR_2. The primary of this transformer has a low loaded Q to provide the relatively broad bandwidth of 0.2 MHz. on a centre frequency of 0.6 MHz. The low Q is obtained by inserting resistors R_{57} and R_{58} across the primary and secondary coils of TR2.

To obtain the frequency to drive the pulse-analog counter, the first intermediate frequency is mixed with the signal from the variable oscillator by transistor T_{12}. The variable oscillator signal is coupled to the emitter of T_{12} through transistors T_{10}, T_{11} and C_{30}. Resistor R_{33} provides amplitude control over the signal injected into the emitter of T_{12} to adjust the input level for best conversion conductance.

The selection of the final difference frequency is achieved by a sixth order low pass Chebyshev filter consisting of L_4, L_5, L_6, C_{33}, C_{34} and C_{35}. The cutoff frequency of this filter is approximately 150 kHz. Design of this filter was simplified by using filter design tables.[31] Proper performance of the filter requires that it be driven by a voltage source and be terminated by proper input and output impedances. Resistor R_{41} provides the 1000 ohms input impedance, since the

output impedance of T_{13} is small. Similarly since the transistor T_{14} has a high input impedance, the output impedance of 2000 ohms is provided by the parallel combination of biasing Resistors R_{43} and R_{42}.

The combination of transistors T_{14} and T_{15} forms a two stage amplifier with a lower 3db point of several tens of cycles achieved by a large emitter bypass capacitor C_{36}. This amplifier boosts the signal to drive the pulse circuit of the counter section. Typical output varies from 3 to 5 volts peak to peak depending on the signal from the monitor oscillator.

In order to minimize interference between high frequency stages, all circuits are decoupled from the positive supply voltage. In addition feedthrough capacitors, for example, C_{19} and C_{39} reduce the 6. and 6.5 MHz signals on this line. Sensitivity of the circuits due to temperature were minimized by exclusive use of NPN silicon transistors and proper DC bias design.

3.7 Pulse Analog Frequency Counter

The frequency of the signal from the amplication stage T_{14} and T_{15} is sufficiently low enough to drive the analog counter directly. As shown in Figure 3.3b this signal drives a Schmitt trigger composed of transistors T_{16} and T_{17}. The square wave output from this stage is differentiated by an RC circuit to obtain trigger pulses for the monostable multi- .

vibrator that follows. The monostable composed of transistors T_{18} and T_{19} provides pulses of constant duration each time it is triggered. By switching in different time constants different pulse durations are possible to accomodate different ranges on one analog readout device. Four time constants are used to provide four frequency ranges. Pulse duration is variable by using potentiometers for R_{64} to R_{67}. The RC networks are switched into circuit by switch SW 1 which, therefore, becomes the frequency range selector for the counter.

Pulse to analog conversion is achieved by current charging capacitor C_{49} through transistors T_{20} and T_{21} switching in parallel. With no output from the monostable the two transistors are off and C_{49} is charged to the supply voltage. When T_{20} and T_{21} are pulsed on, the capacitor discharges through the transistors for the duration they are on. For a given pulse duration, the voltage on the capacitor reaches some direct current equilibrium value when the average charging and discharging rates are equal. The average charging current is therefore directly proportional to the frequency and is measured by meter M_1. Since M_1 has a one milliampere d.c. movement, different frequency ranges are covered by changing the duration that T_{20} and T_{21} are on. This, as explained, is done by the monostable multivibrator; the greater the frequency range to be covered, the shorter the time duration. Using this technique M_1 covers the frequency ranges of 1KHz, 5KHz, 10KHz

and 50KHz. Range switching, as indicated, is by switch SW 1.

The total resistance of meter M_1 and resistors R_{73a} and R_{73b} is adjusted to 5000 ohms. Thus for full scale deflection of the meter the voltage drop across this resistance is 5 volts. This voltage is available at the rear of the monitor for thickness control purposes. The voltage across R_{73b} is also made available for recorder attachment. For full scale deflection of M_1 the output across R_{73b} is 10 millivolts.

3.8 The Rate Circuit

For a zero to full scale deflection of meter M_1 the voltage on the capacitor changes linearly from 15 to 10 volts irregardless of the frequency range being covered. Consequently, the voltage on the capacitor C_{49} has a negative ramp function characteristic with deposition. By differentiating this voltage, a signal proportional to rate of change of frequency and hence rate of deposition can be obtained.

The simplest way to perform this operation is by use of an RC operational differentiator circuit. In Figure 3.3b the basic operational differentiator consists of a Philbrick transistorized operational amplifier (Model PP85AU) combined with C_{51} and R_{74}. C_{51} has a value of 10 microfarads and R_{74a} a value of 1.0 megohms giving an RC time constant of 10 seconds. This means that for a ramp voltage input with slope -0.50 volts/ sec. the differentiator output is 5 volts.

To stabilize the differentiator and reduce its sus-

ceptibility to noise R_{74b} is added in series with C_{51} and
C_{52} in parallel with R_{74a}.[32,33] The diode-resistance network
in parallel with the feedback resistor R_{74a} limits the output
of the differentiator to -0.1 to 5.5 volts to prevent the
amplifier from being driven heavily into saturation when sub-
jected to sudden input voltage transients.

The output of the differentiator is indicated by
ratemeter M_2, which has a 100 microampere full scale move-
ment. Resistor R_{76} and R_{77} are two calibration resistors en-
abling M_2 to cover two rate ranges. The second range is ten
times more sensitive than the other. This second range en-
ables more accurate readings of low rates of deposition.
Zeroing of M_2 is achieved by R_{79} and R_{80} which adjust the
off-set current of the operational amplifier. Capacitor C_{54}
is placed across M_2 to smooth out small fluctuations and faci-
litate easier reading of the meter. For purposes of deposition
control, the full output voltage of the differentiator is
available at the rear plug-in-terminal.

3.9 Power Supply

The power supply for the monitor is shown in Figure 3.3b.
Two regulated voltages are available, 15 and -15 volts. Un-
regulated positive and negative voltages are obtained by
using a full wave bridge rectifier across a transformer with
a grounded centre tap. The 15v line supplies all oscillators
and pulse circuits. Since this line must be well regulated
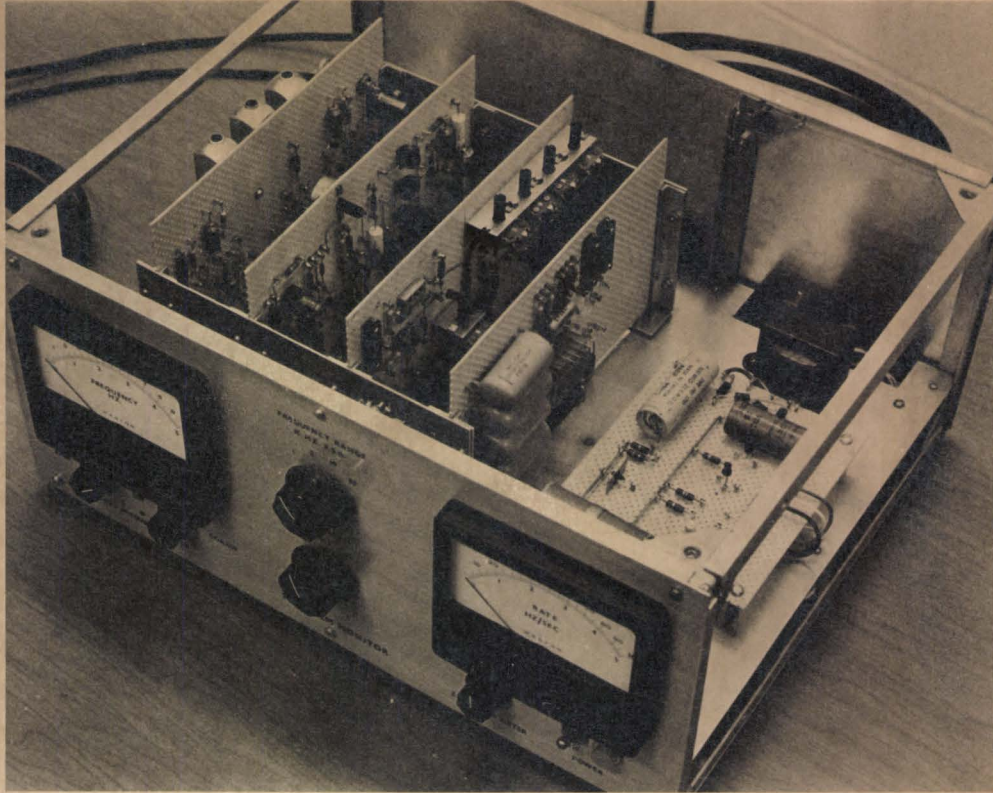
Figure 3.4

Internal Construction

of Film Thickness Monitor

to obtain good frequency stability and maintain calibration in the analog counter, a series voltage regulator with a zener reference is used. Line regulation is for $\pm$ 15% of the a.c. supply voltage. For the -15 volt supply adequate regulation is obtained by using a zener shunt regulator. C_{55} across the output of the supply helps to decrease the high frequency output impedance of the supply. The total power consumption including the power supply is 2.5 watts.

3.10 Construction

The complete film thickness monitor, with the exception of the monitor oscillator is contained in a $16\frac{1}{2}"x12"x7"$ aluminum frame as shown in Figure 3.4. All electronic components are mounted on five separate "vector boards" by means of "push through" terminals. The circuit boards are edge mounted in a rack and connections between boards are by printed circuit edge connectors, thereby facilitating easy removal for inspection and repair. Both the frequency and the rate meter are mounted on the front panel together with the range switches and meter zeroing controls. Plug in terminals for connecting the monitor oscillator unit, chart recorder, and thickness and rate controller are mounted on the rear panel.

Figure 3.5 shows the covered monitor together with the 6.5 MHz monitoring oscillator. The aluminum box housing the oscillator is attached directly to a vacuum feedthrough, which contains the insulated conductors by means of which the monitor-

Figure 3.5

Front Panel View of Film Thickness Monitor

Together with Monitor Oscillator and Connecting Cables

ing crystal located in the vacuum chamber is connected to the oscillator circuit. The oscillator is mounted directly below the base plate of the vacuum chamber by means of this feedthrough. Such an arrangement permits the shortest leads between the monitoring crystal and the external mounted oscillator circuit. Adequate shielding is also provided since both the feedthrough and box are grounded. The power for the oscillator is supplied from the main unit via ten feet of twin-lead shielded conductor. The high frequency signal from the monitor oscillator is fed to the main unit through 10 feet of 50 ohm shielded coaxial cable.

3.11 Complete System for Controlled Deposition

With the D.C. voltages proportional to deposition thickness and rate available from the monitor, the unit can be used, together with the appropriate control equipment, to control the deposition during an evaporation cycle.

A complete evaporation control system was set up by combining the above monitoring unit with some commercially available apparatus. This consisted of an Edwards High Vacuum Automatic Controller (Model 1, Code No. D 16701) together with a 4.5 KVA Silicon Controlled Rectifier stack (Edwards High Vacuum Code No. D 16704). The system is operated with an Edwards 19E vacuum evaporation unit. The complete system is shown in Figure 3.6. Since details of this control system have been given in the literature [34,35] and operation of the
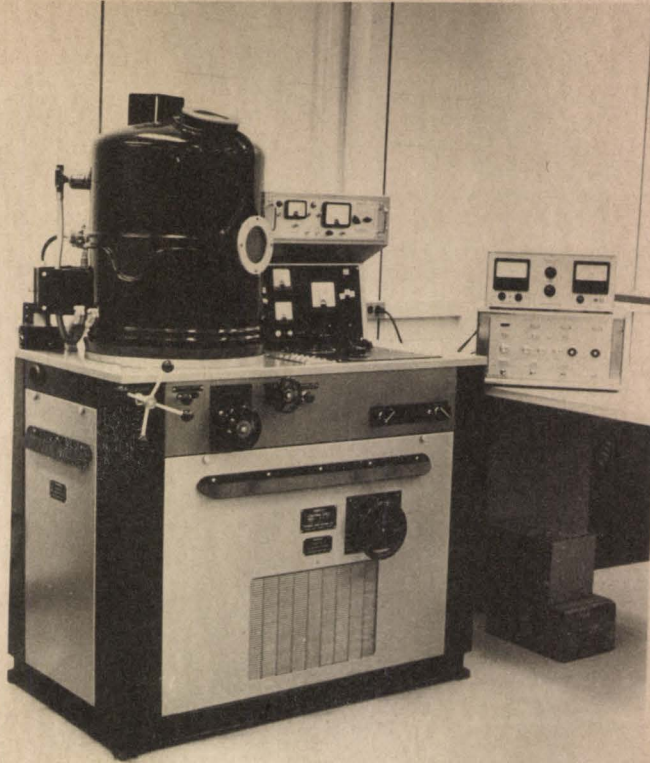
Figure   3.6

Complete Automatic Deposition

Control System
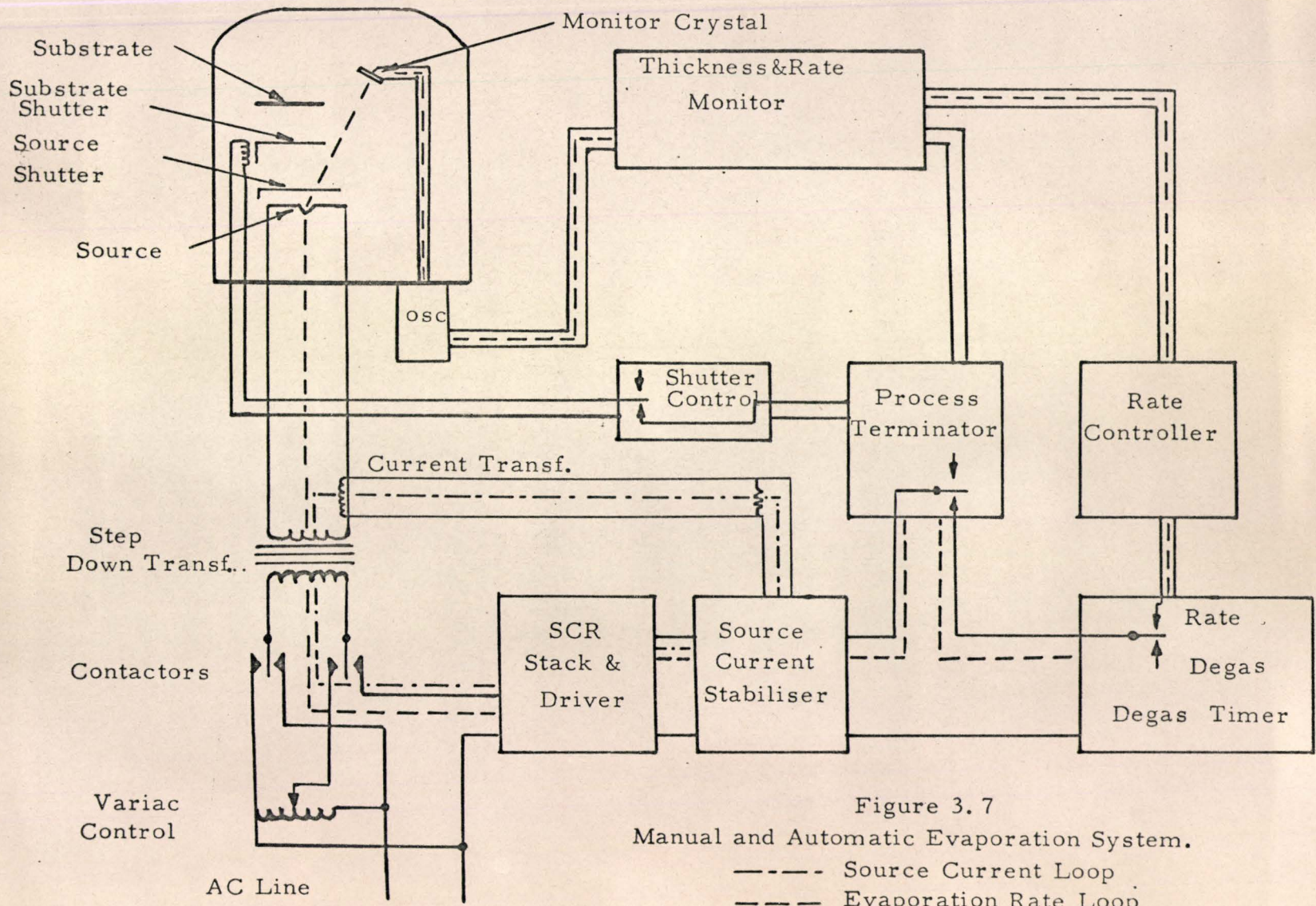
Figure 3.7

Manual and Automatic Evaporation System.

—·—·— Source Current Loop

— — — Evaporation Rate Loop

controller adequately described in the accompanying manual,
(Reference M 11 656/5) only a very brief description of the
essential operation is given here.

Figure 3.7 shows the above control apparatus in block
diagram form. A typical evaporation begins with the degas
timer set to control the silicon controlled rectifier (SCR)
power supply. Under this control the SCR supply applies an
increasing current to the evaporation source boat and contents,
heating them slowly up to the degassing temperature and then
holding this temperature until degassing is complete. The
rate of rise of the initial degassing current, the degassing
current, and the total degassing time can be varied to accomodate
various sources and materials. At the end of the total de-
gassing time, the system automatically switches over to the
evaporation rate controller. At the same time the substrate
shutter is opened. In the evaporation rate controller, an
output signal from the rate monitor is compared with a re-
ference rate and the amplified error signal fed to the SCR
supply. The maximum current of the rate controller is vari-
able and must be used to obtain evaporation rate stability.
Stability is a problem because of the unpredictable thermal
delays due to different evaporation sources and materials.

A second feedback loop exists which stabilizes the
evaporation source against a.c. line voltage fluctuations.
In addition the source current stabilizer can be used alone
to drive the SCR supply. With this mode of control, reason-

ably constant rates of evaporation can be obtained with a number of materials evaporated from resistance heated sources.[36]

Two additional modifications were included in the system shown in Figure 3.7 to provide greater versatility and ease of operation. The first is that manual variac control for the source current was retained in case of SCR supply failure. The switching over from one to the other is achieved by two sets of contactors operated sequentially by a rotary switch. This arrangement protects the SCR supply since the driving circuit should be turned on one second before the load is switched in. Secondly, the system contains two shutters. The source shutter, operated manually can completely shut off the evaporant stream. The substrate shutter, on the other hand, completely covers only the substrate, leaving the sensor crystal exposed to the evaporant stream when the source shutter is open. The substrate shutter can be operated manually or automatically by a signal from the process terminator. The advantage of this arrangement is that it permits a deposition rate to be set and allowed to stabilize prior to exposing the substrate.

CHAPTER 4

Procedure for Thickness Calibration of Monitor and
Rate Controlled Evaporations

4.1 Introduction

The monitor as described in the last chapter measures the film thickness and the rate of deposition indirectly in terms of frequency changes. To be more meaningful, these readings in hertz and hertz/second, must be converted to anstroms and angstroms/second. As pointed out in the second chapter, the required conversion factors can be calculated provided a number of important parameters of the particular evaporation system are taken into account. However, an experimental calibration may sometimes prove easier to perform because of uncertainties in the system. In this chapter the experimental procedure used to calibrate the system both in terms of frequency units and thickness units is described. The results can then be used to verify the theoretical calculations.

4.2 Frequency Calibration of Frequency Counter

The frequency counter, meter M_1, covers four frequency ranges: 1 KHz, 5 KHz, 10 KHz, and 50 KHz. Switch SW_1 selects

48

the appropriate range by switching one of four time constants
into the monostable multivibrator. In order to use the meter
each range must first be individually calibrated. This cali-
bration involves adjusting the average D.C. current through
M_1 to exactly one milliampere (the full scale deflection cur-
rent), as the multivibrator is switched at the frequencies of
1, 5, 10, and 50 kilohertz respectively.

From a practical standpoint, the following calibration
procedure was found to give the best results:

First, the positive supply voltage is checked and ad-
justed to exactly 15 volts dc. Next, the variable frequency
oscillator is adjusted to obtain a second I.F. of 10 KHz.
This frequency is accurately measured by monitoring the input
to the Schmitt trigger with a digital frequency counter (Hewlett
Packard Type 3734A). Range switch SW1 is then set to the 10
KHz range and resistors R_{66} and R_{69} simultaneously adjusted
until M_1 shows a full scale deflection. R_{66} adjusts the pulse
duration, while R_{69} is adjusted so that the required pulse du-
ration is small compared to the time interval (10^{-4} seconds)
between pulses. Once R_{69} has been set for this range it is
not adjusted further for the others, since this would offset
the calibration of 10 KHz range. In a similar manner, with
the exception of further adjustment to R_{69}, the 1, 5, and 50
KHz ranges are calibrated by adjusting R_{67}, R_{65}, R_{64}, respective-
ly.

The frequency counter is now calibrated in hertz to

measure the frequency changes of the monitor crystal. The above calibration should be checked periodically to assure accurate frequency measurements.

4.3 Frequency Calibration of the Rate Meter

The output of the differentiator of the rate circuit is $-RC \frac{dv}{dt}$, where RC is the time constant, and $\frac{dv}{dt}$ the time rate of change of the input voltage. The values of R and C have been selected to give a time constant of 10. The error in the time constant can be corrected for by adjusting the rate calibration resistors R_{76} and R_{77}.

The maximum output of the differentiator is 5.0 volts, corresponding to a ramp voltage input of -0.5 volts per second. M_2 has a full scale deflection current of 100 microamperes. Thus, to calibrate this rate range R_{76} is adjusted so that the internal resistance of M_2 combined in series with R_{76} is equal to 50 Kohms. For voltage inputs less than -0.05 volts per second the ratemeter is switched in series with R_{77} and the total series resistance adjusted to 5 Kohms. This latter range is ten times more sensitive and permits more accurate measurements of low deposition rates.

The above calibration of the deposition rate meter M_2 was then checked during a typical deposition. This can be done by two different and quite accurate procedures. In the first method the reading on M_2 is compared with the change in frequency for 10 second intervals as measured by a digital counter (Hewlett Packard 3734A) connected as before to the

input of the Schmitt trigger. The counter provides a measure of the deposition rate in Hz/second averaged over 10 second intervals. The second method involves attaching a chart recorder and plotting the change in frequency with time. The slope of this curve is equal to the rate of deposition. Final adjustments to R_{76} and R_{77} based on the above comparisons complete the ratemeter calibrations.

It is important to realize that the thickness monitor as calibrated above provides a measure of the thickness of the deposited film indirectly in terms of an equivalent frequency change, measured in hertz, of the sensor crystal. Similarly, the rate of deposition is given in equivalent hertz/second.

Furthermore, it is important to realize that the reading on the ratemeter M_2 is dependent upon the frequency range to which M_1 has been switched. This is illustrated in Table 3 below. The table shows the maximum rates measurable by the two ranges of the ratemeter for each thickness range.

TABLE 3

Frequency Range and Corresponding Rate Ranges

Thickness	Maximum Measurable Rate	
Range	x1.0 Range	x0.1 Range
KHz	Hz/sec.	Hz/sec.
1	100	10
5	500	50
10	1,000	100
50	5,000	500

To facilitate reading of the rate of change of frequency, meters M_2 and M_1 have corresponding scale markings. The rate of deposition can thus be obtained at a glance by keeping the maximum rates per range in mind. Otherwise the following formula can be used:

$$\text{Rate} = \frac{\text{Meter deflection}}{\text{Full scale deflection}} \text{ x } \frac{\text{frequency range}}{10} \text{ x } \frac{\text{Hz.}}{\text{sec.}} \qquad \text{Eqn. 4.1}$$

To obtain the rate reading when using the x0.1 range the frequency range in the above formula is divided by 100 instead of 10.

4.4 Thickness Calibration of Monitor in Angstroms

The procedure for thickness calibration of the monitor consisted of the deposition of a series of thin films on separate substrates and carefully recording the resulting frequency change of the monitor crystal. The thicknesses of the deposited films were then measured directly and correlated to the measured frequency changes. Two methods for determining the thickness of the deposited film can be used. The thickness of the film were found by careful weighing with a microbalance. Or, they were measured optically by means of a multiple beam interferometer.

Silver films were used for the thickness calibration. Silver was chosen because it was readily available and is also easily evaporated from a molybdenum source. Its density of 10.5 gm/cm^3 is relatively high and hence the frequency change

is large permitting a more accurate measurement. Freshly
deposited silver also does not oxidize readily; hence, it is
unnecessary to make an immediate thickness determination.
Finally, the high reflectivity of silver films makes them
ideally suited for interferometric thickness determinations.

Microbalance Weighing

When using the weighing technique, clean glass sub-
strates were accurately weighed before and after deposition
to determine the weight of the film. Assuming bulk density
then the average thickness of the film would be calculated from

$$t = \frac{m}{p_m A}$$

where m is the mass of the deposited film p_m the density of
the film and A the area of the deposition. One of the draw-
backs to this method is that the assumption of bulk density
is not valid for thin films and, furthermore, the actual den-
sity is not easily determined. In addition while making actual
calibration depositions, it was found that the glass substrate
would tend to chip during mounting and demounting, thereby
changing the weight of the substrate. This resulted in a large
error in the weight of the deposited film. On account of the
above difficulties, it was decided to abandon this approach in
favour of determining the film thickness optically.

Multiple-Beam Interferometer

To measure the thickness of a thin film optically with

an interferometer a well defined step in the film is required.
A narrow channel is sometimes helpful when the glass surface
is not very flat. To avoid correcting for the difference of
reflectivity between the film and the substrate, a second
opaque film is deposited over the step. A small comparator
plate is then placed over the step in the film. This arrange-
ment is shown in Figure 4.1. When a collimated beam of white
light is shone onto the film through the comparator plate,
fringes are formed by interference between the two metalized
glass plates.

These fringes can be viewed by means of an interference
microscope situated above the comparator plate and a constant
deviation wavelength spectrometer. When the microscope is lo-
cated above the channel in the thin film the fringes appear as
shown in Figure 4.2. The steps in this diagram are associated
with the steps of the channel in the film.

If d and d' are the distances between the top and
bottom of the channel and the comparator plate as indicated in
Figure 4.1 then it can be shown that the thickness of the de-
posited film is

$$t = \frac{n}{2} \Delta \lambda_2.^{37} \qquad \text{Equation 4.2}$$

In the equation n is the order of the interference and is a
whole number. It is found from the relation

$$n = \frac{\lambda_2}{\lambda_1 - \lambda_2} \qquad \text{Equation 4.3}$$
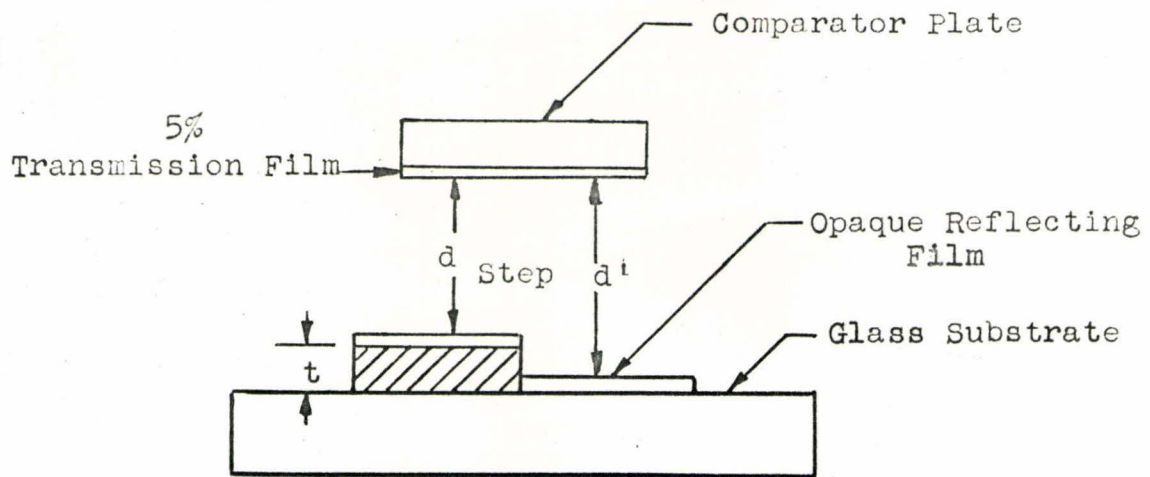
Figure 4.1

Film Sample Preparation for Thickness Measurement with
Multiple Beam Interferometer
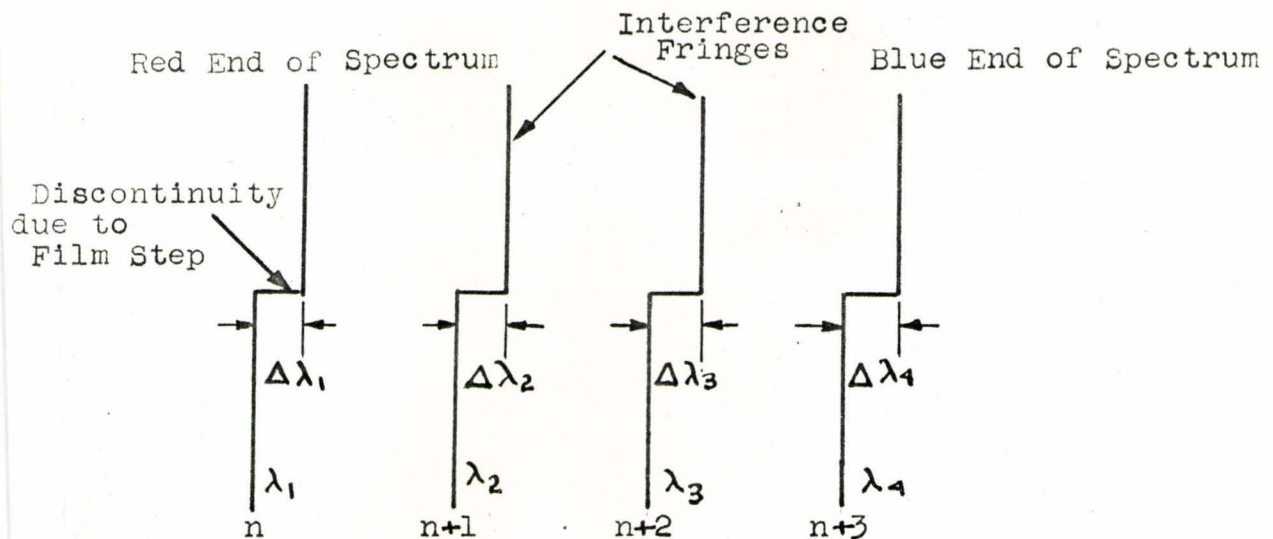
Figure 4.2

Fringe Pattern Observed in Multiple Beam Interferometer

Now λ_1, λ_2 are the wavelengths of two adjacent fringes as shown in Figure 4.2 and $\Delta\lambda_2$ is the height of the step in the fringe. Numerical values for λ_1, λ_2 and $\Delta\lambda_2$ in angstroms are read from the wavelength drum of the spectrometer. In order to minimize the error due to phase changes at reflection, the order n should be chosen to lie between 4 to 8. At n = 8 this error is 0.5% whereas at n= 4 it is 3%.

In the thickness measurements made, a Thin Film Measuring Interference Microscope (Hilger Watts N 130) was used in conjunction with a Constant Deviation Wavelength Spectrometer (Hilger Watts D9003). The accuracy of these instruments is quoted by the manufacturer to be $\pm$ 25 angstroms.

4.5 Sample Preparations for Thickness Calibration

The Edwards 19E vacuum evaporation unit with which the thickness monitor is to be used, contains a rotating micro-circuit jig. This jig can hold six substrates and six masks and evaporate from six separate sources. Since the jig can be manipulated from outside the vacuum chamber, films can be evaporated on all the substrates through a sequence of masks without breaking the vacuum.

To prepare for thickness calibration a set of six glass substrates were cleaned by first scrubbing with detergent, then boiling in aqua regia for fifteen minutes. After rinsing with distilled water, the substrates were allowed to dry. The substrates were then mounted into holders and inserted into the

rotating jig. Two metal masks were required to evaporate films suitable for the interferometric thickness determination. The patterns are shown in Figure 4.3; the actual masks were handcut from thin brass shim stock.

With the masks, substrates, and silver charge in place, a clean quartz crystal was placed into the holder and the monitor turned on. The vacuum chamber was then sealed and pumping down procedure initiated.

During the pump down the monitor was on to allow the oscillator time to stabilize. When the pressure had reached 3×10^{-5} torr the evaporations were begun.

First, a film of silver was evaporated on the substrate through mask No. 1. With this mask a 1x0.5 inch film with a 7 mil wide channel down the centre was produced. The resulting frequency change of the monitor crystal was carefully recorded. Mask No. 2 was then rotated into position and a second silver film was deposited over the first. Again the frequency change of the monitor crystal was carefully recorded. This second film was made sufficiently thick to allow enough light to be reflected from the bottom of the channel to get a good presentation of the interference fringes in the spectrometer telescope.

Two sets of six thin silver films of increasing thickness were deposited as described above. It was decided to get an accurate measurement of frequency changes as possible; therefore, the monitor crystal frequency changes were directly

7 mil wire
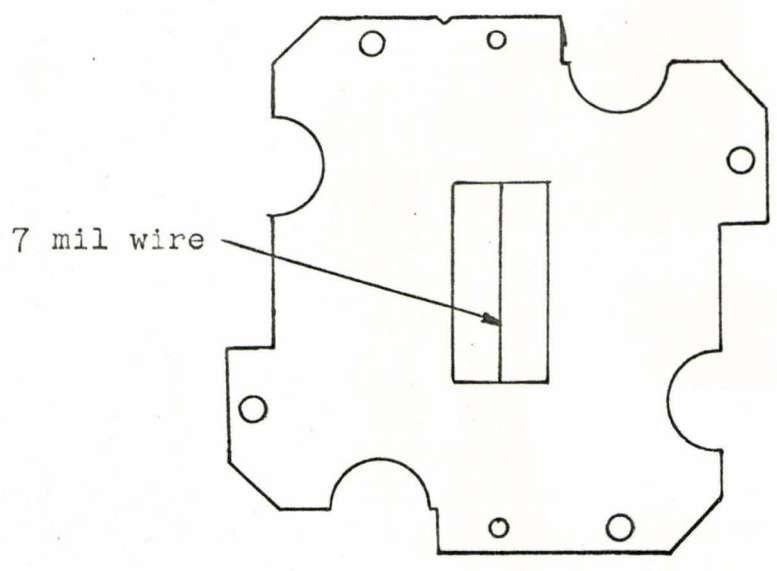
Mask No. 1
(Actual size)
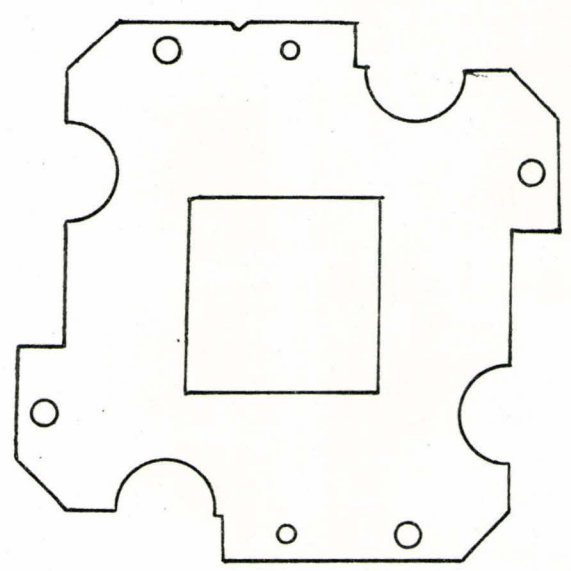
Mask No. 2
(Actual Size)

Figure 4.3

Metal Masks Used for Evaporation of Silver Calibration
Film.

measured with a digital frequency counter. In addition to recording the frequency changes due to the deposited silver films, the cumulative frequency change of the monitor crystal was also recorded.

The thickness of each deposited silver film was measured with a multiple-beam interferometer. The results were then used to plot a calibration curve for the monitor. Calculations based on this data were also made to verify the results obtained in chapter two. These results are presented in the next section.

4.6 Controlled Evaporations of Thin Films

The basic operation of the system for controlled evaporation of thin films has been described in section 3.11. The instructions for using the Edwards automatic rate controller (Model 1 Code No. D16701) are outlined in the operations manual (M1165615) which is supplied with the unit, hence, no detailed procedure will be given here. Proper operation of the system requires a basic understanding of how the system functions and experience gained from working with the system. The optimum setting of the maximum degassing current and time, for example, varies with material and evaporation source, consequently, no fast rules can be given. However, once an acceptable evaporation cycle has been worked out, it can be used again and again with repeatable results.

In the evaluation of the controlled evaporation system,

the main criterion was to be its ability to maintain constant evaporation rates and deposition thickness. To this end a number of materials used for thin film studies or thin film electronic devices were evaporated with and without rate control. Chart recordings of the frequency changes (thickness) were made and traces of these are shown in the next section. In one series of tests an artificial voltage fluctuation was introduced and the evaporation rate recorded with and without rate control.

The Edwards control unit is also capable of providing film thickness control. The evaporation is terminated when the preset thickness has been reached. The calibration of the thickness control potentiometer is described in the operating instructions (M11656/5) and is not given here. The stability of the thickness control is quoted by the manufacturer to be $\pm 2\%$ of the frequency meter setting. This value was accepted per se and no tests performed to verify it.

CHAPTER 5

Performance of the Thin Film Thickness Monitor as an Instrument
for Measuring and Controlling Deposition from a Resistance
Heated Source

5.1 Introduction

In this chapter the performance of the thickness monitor
will be evaluated on the basis of the results obtained from the
tests described in the previous section. The calibration data
obtained from these tests is presented to be used with the moni-
tor when making thin film measurements.

5.2 Calibration Data

After the calibration of the frequency counter, meter
M_2, the linearity of each range was measured. The data is shown
tabulated in Table 4 for each frequency range. The left hand
column gives the meter setting, while the adjacent four columns
give the corresponding frequency on each range as measured by a
digital counter. The results in Table 4 indicate that the
accuracy of the frequency counter is approximately 1% of the
full scale deflection over each frequency range. This accuracy
is quite repeatable after having carefully performed the cali-
bration as outlined in section 4.2. The best results were ob-

tained by calibrating $\frac{1}{2}\%$ high at full scale deflection. Since
small changes in component value occur with time, the calibra-
tion of M_2 should be checked periodically and adjustments made
if necessary.

TABLE 4

Linearity of the Ranges of Frequency Meter M_1

Meter Reading	Frequency Ranges			
	1 KHz.	5 KHz.	10 KHz.	50 KHz.
0.1	91	439	896	4,680
0.2	191	946	1,892	9,560
0.3	290	1,449	2,891	14,728
0.4	394	1,968	3,907	20,145
.5	494	2,472	4,931	24,923
.6	598	2,996	5,996	30,067
.7	698	3,498	7,005	35,035
.8	804	4,038	8,062	40,450
.9	908	4,551	9,087	45,874
1.0	1,014	5,078	10,139	51,198

5.3 Data for Thickness Calibration of Monitor

The correlation between the frequency change of the monitor crystal and the thickness of the film deposited on the substrate has been obtained experimentally. The procedure to obtain this data has been outlined in section 4.3. Table 5 below shows the frequency changes of the monitoring crystal together with the film thickness for 12 silver films. The film thicknesses as shown in the table represent the average of three values measured in the middle and near each end of the narrow channel as shown in Figure 4.3. The thickness of the substrate film is a maximum at the centre and decreases radially as indicated by equation 2.20. Thus an average value is more representative of the film thickness at any arbitrary point; moreover, errors in the interferometer measurements are averaged out.

TABLE 5

Calibration Data for Thickness Monitor Relating Substrate Film Thickness to Frequency Change of the Monitor Crystal

Film No.	Δf Hz.	t_s Å	$C_t \frac{gm}{cm^3} \frac{Å}{Hz.}$
1	3,157	957	3.18
2	7,126	2150	3.17
3	12,020	3380	2.95
4	15,393	4250	2.90
5	20,211	5570	2.89
6	25,673	6790	2.77
7	2,014	563	2.92
8	4,322	1095	2.68
9	7,271	1895	2.74
10	10,225	2560	2.73
11	15,209	3670	2.53
12	17,600	4670	2.79

Heat Shield

Monitor Crystal

0.635cm Aperture

Substrate
5cm

3.5cm

∅

r= 21.0cm

h=14.2cm

10.2cm

Cos ∅ = 0.945

Small area directed
surface source
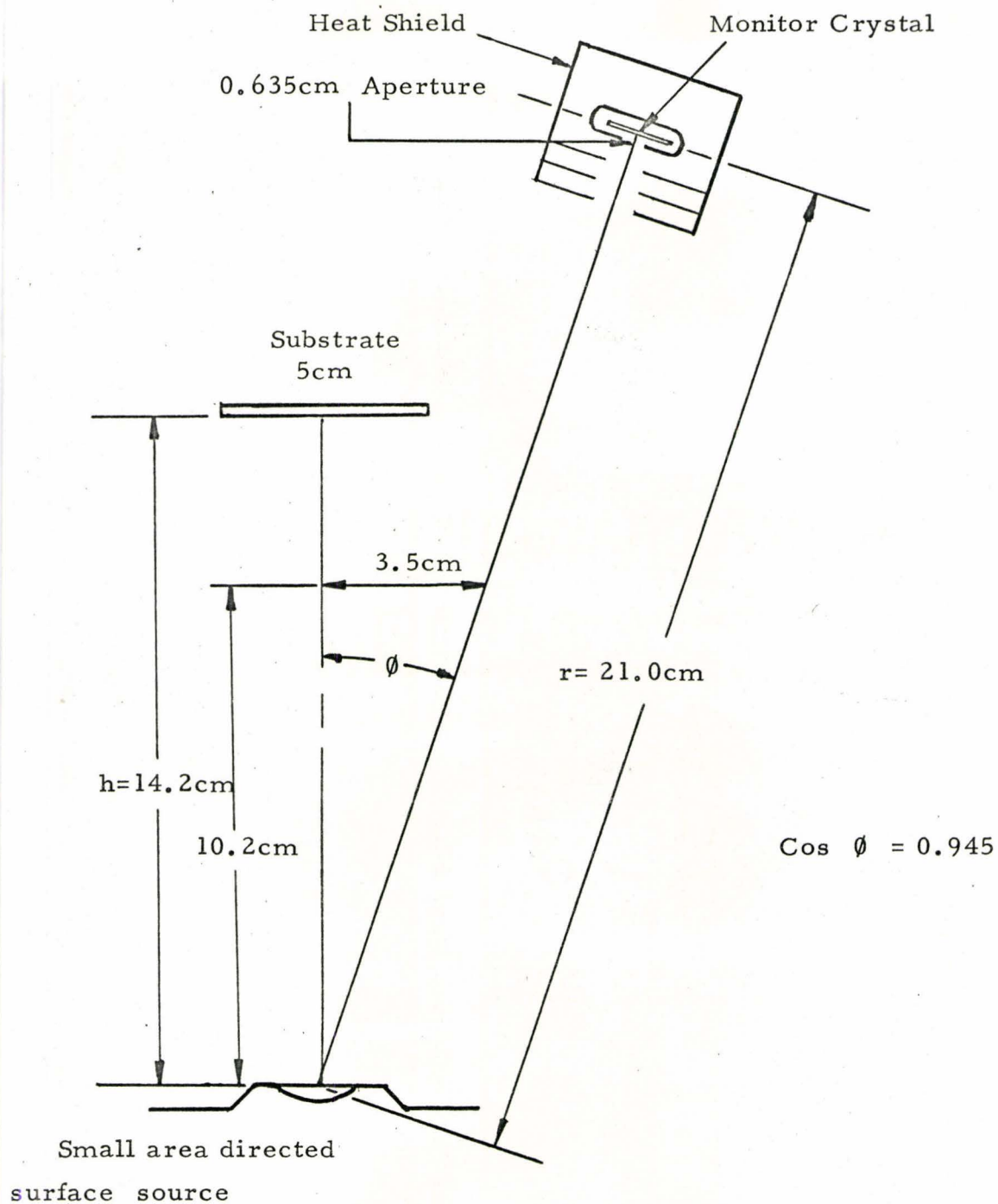
Figure 5.1

Source, Substrate and Monitor Geometry in Vacuum Chamber of
Edwards High Vacuum 19E Evaportation Unit.

Figure 5.2

Cumulative Change in Frequency of Monitor Crystal with Cumulative Thickness of Silver Substrate Film

Density of Silver 10.0 g/cm³

0.635 cm dia. aperture

Substrate Film Thickness, Microns
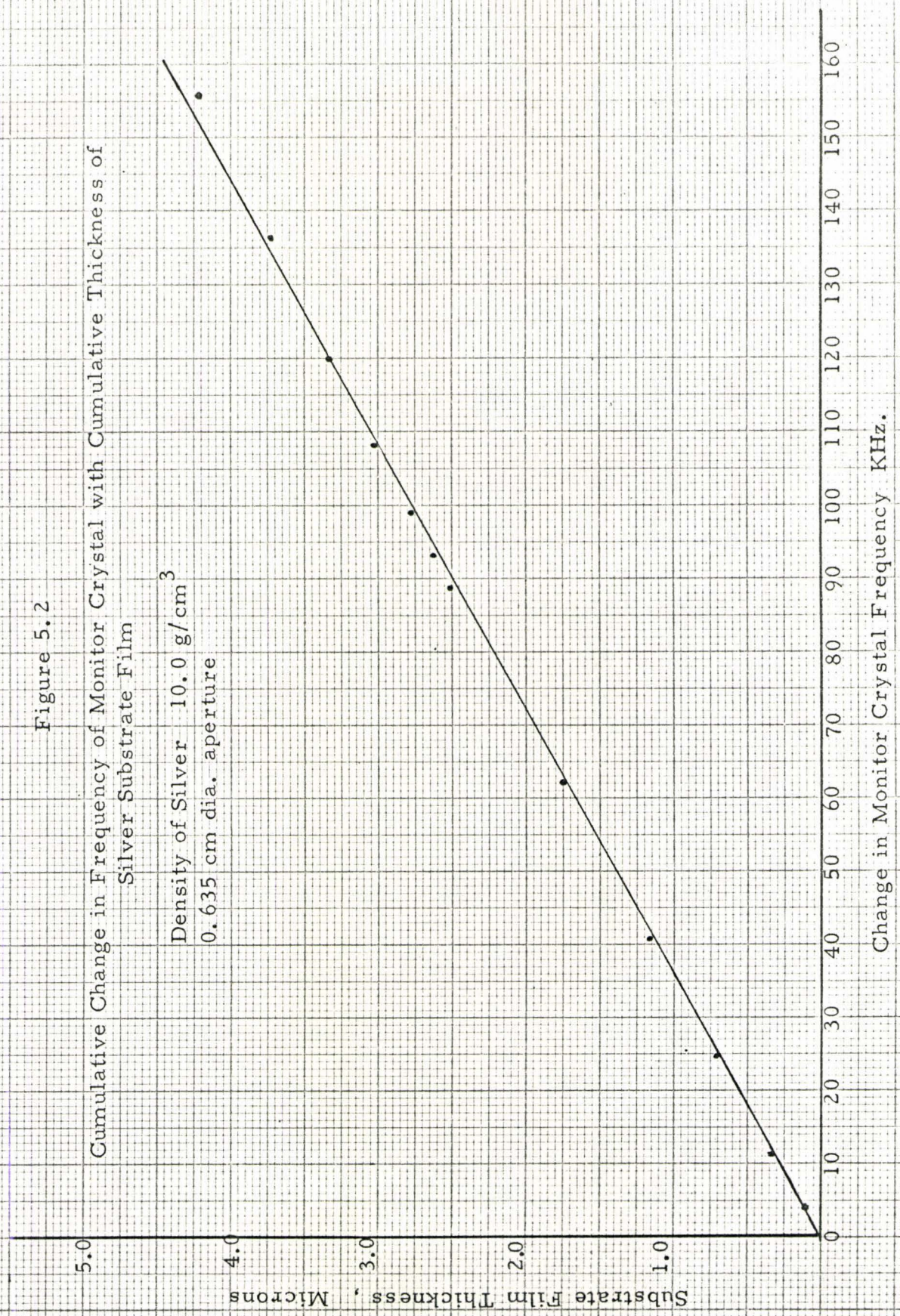
Change in Monitor Crystal Frequency KHz.

By using the data in the second two columns of Table 5
a calibration constant can be claculated by using equation 2.8.
Replacing C_f by C_t in equation 2.8 and rewriting, then

$$C_t = \frac{p_m t_s}{\Delta f} \quad \frac{gm \; \mathring{A}}{cm^3 \; Hz.} \qquad \text{Equation 5.1}$$

The factor C_t could be defined as the "thickness de-
termination sensitivity". From the data in the table the mean
C_t for the 6.0 MHz crystal monitor is 2.85 ± 0.05 gm $\mathring{A}/cm^3$ Hz.
This value has been calculated by using the density of silver
as being 10.5 gm/cm^3 and is valid only for the evaporation
source and geometry shown in Figure 5.1.

A cumulative plot of the data has also been made and
is shown in Figure 5.2. The graph in this figure shows the
continuous frequency change of the monitor crystal as the twelve
films of Table 5 were deposited. Corrections have been inserted
in this plot for additional frequencies and thickness changes
due to the thin silver overlay films required for interfero-
metric thickness measurements. The plot indicates that the
AT 6.0 MHz monitor crystal can be employed up to a total fre-
quency change of at least 150 KHz before replacement. This
is equivalent to depositing 42,000 Angstroms of silver on the
substrate.

The experimentally determined mean value of C_t for
silver can be used to calibrate the monitor crystal for use
with other materials. If the density of the material is known,
then substituting for p_m in Equation 5.1 the substrate thick- .

ness t_s for any frequency change Δf can be calculated. In Table 6 the film thickness equivalent to a Δf of 1,000 Hz has been tabulated for a number of common materials. Again results in the table are valid only if the material is evaporated from a directed small area source and the substrate and crystal geometry of Figure 5.1 are used. If other conditions prevail then corrections must be made to the data in Table 6; otherwise, there may be significant differences between the actual and the indicated measurements.

TABLE 6

Film Thickness corresponding to 1000 Hz for Source, Substrate and Monitor Geometry of Figure 5.1

Material	Density gm/sec	Film Thickness for Δf = 1000 Hz $\overset{\circ}{A}$	Deposition Rate for 10Hz/sec $\overset{\circ}{A}$/sec
Aluminum	2.67	1070	10.7
Silver	10.5	272	2.72
Gold	19.3	148	1.48
Bismuth	9.67	295	2.95
Lead	11.0	260	2.60
Cadmium Sulphide	4.82	592	5.92
Silicon Monoxide	2.20	1290	12.9
Silicon Nitride	3.44	830	8.30

5.4 Calibration Data For Ratemeter

The calibration of the ratemeter is essentially complete when the adjustments outlined in section 4.3 have been

made. Consequently it is only necessary at this point to con-
vert the rate of change of frequency in Hz/sec. to Å /sec. In
column 4 of Table 6 the rates of deposition equivalent to 10Hz/
sec. have been tabulated for a number of materials. This data
is based on the experimental calibration made for the system
with silver.

In section 4.3 it was also indicated that the reading
of the ratemeter is dependent upon the frequency range of M_1.
The maximum rates for each range in terms of frequency are shown
in Table 3. However, the actual deposition rates in Å/sec. are
also, as shown in Table 6, a function of material density. The
maximum deposition rates measurable by the monitor for each
thickness ranges for silver are shown in Table 7. This table
gives a good indication of the wide range of rates that are
measurable.

TABLE 7

Maximum Deposition Rates for Silver Measurable by the

Ratemeter

Frequency Range	Rate Å/sec.	
	1.0 Range	0.1 Range
1KHz	27.2	2.72
5KHz	136	13.6
10KHz	272	27.2
50KHz	1360	136

One of the important things to note in Table 7 is the
considerable overlapping of deposition rates resulting from the

use of two rate ranges. This is a definite advantage when
it is desirable to deposit a relatively thick film at low de-
position rates. Such a situation might arise when depositing
such semiconductor materials as, for example, cadmium sulphide
for thin film active devices.

5.5 Comparison between Calculated and Experimental Calibration
Constants

In the Edwards 19E vacuum chamber the monitor crystal
is further away from the evaporation source than the substrate.
Furthermore, the surface normal of the crystal makes an angle $\emptyset$
with the surface normal of the source as shown in Figure 5.1.
Due to these two factors the thickness on the crystal is less
than the film deposited on the substrate.

The actual thickness relationship between the two films
is given by Equation 2.18, namely,

$$\frac{t_s}{t_x} = \frac{h^2}{r^2 \cos \emptyset \cos \theta} . \qquad \text{Eqn. 2.18}$$

Substituting the numerical values of Figure 5.1 in the above
equation then
$$t_x = 0.433 \ t_s.$$
Thus the film deposited on the crystal has slightly less than
half the thickness of the film deposited on the substrate.

It also follows from this result that the mass/area
ratio of the crystal film to the substrate film is also 0.433.
Therefore, less mass is deposited on the crystal and the sen-

sitivity of the monitor crystal has been effectively halved. On the other hand, because the mass loading of the crystal has been approximately halved, the film thickness measurable by the crystal has been effectively doubled.

In chapter two the expression $C_f = \dfrac{f_o{}^2 K}{pqN}$, called the "mass determination sensitivity" was derived . Now C_f provides a measure of the frequency change that a quartz crystal undergoes when a unit mass of material is uniformly deposited over its active area. If the entire active area of the crystal is covered C_f reaches its theoretical maximum and the constant K is unity. The calibration data for silver and the data from Figure 5.1 can be used to calculate the experimental sensitivity.

Correcting for the geometry and cosine effect of the small area directed surface source the experimental mass determination sensitivity for the quartz crystal is

$$8.12 \pm .14 \times 10^7 \ \frac{Hz \ cm^2}{gm} .$$

From Table 1, the theoretical value of C_f for a 6.0 MHz At cut crystal is
$$8.15 \times 10^7 \ \frac{Hz \ cm^2}{gm} .$$

Thus K, the ratio of the measured sensitivity to the theoretical sensitivity has a value of $0.996 \pm .02$.

This value of K verifies that within the experimental error the area of deposition, which is 0.25 inches in diameter, is sufficiently large to cover the active area of the crystal. Further-

more, it indicates that the maximum theoretical sensitivity can indeed be reached in practice.

The most important consequence that follows from the near unity value of K, however, is that the experimental calibration procedure as performed with silver is not necessary. The required calibration constants can be calculated by taking into account the source evaporation characteristics, the source crystal and substrate geometry, and assuring that deposition on the crystal covers the entire active area.

Although there is good agreement between the experimental and theoretical data, it must be remembered that it is only valid for the change of 150 KHz. of the resonant frequency of the quartz. This is approximately 2.5% of f_0. Within this frequency change, thickness measurements based on a theoretical or an experimental calibration can be accepted with a high confidence level. It is not recommended that the crystal be used beyond this range as the mass loading effect may deviate considerably from linear behaviour. Furthermore, a stage of erratic behaviour including cessation of oscillations may occur at some point beyond this change. Such behaviour would be undesirable during a critical deposition.

When discussing the nonlinearity of the mass loading effect of the quartz crystal in chapter two, it was shown that there is a 1% deviation in film thickness for every 0.5% change in the resonant frequency. This deviation was shown to be a result of the decreasing sensitivity with decreasing frequency.

This effect would manifest itself as a small but continuous increase in the slope of the cumulative thickness versus frequency plot of Figure 5.2.

For a change in frequency of 155 KHz., the deviation should be approximately 5%. Allowing for experimental error in the data, the results in Figure 5.1 do not show such a change. There is in fact an indication of an increase in the sensitivity as indicated by a slight decrease in the slope of the actual experimental curve.

The reason for this discrepancy may be partially attributed to the fact that with increasing thickness, the deposited film begins to store sufficient potential energy to affect the sensitivity. Thus the assumption $\Delta C_{nn} = 0$ used in deriving equation 2.8 no longer holds. If it is assumed that the film does store potential energy, then it can be shown that the crystal sensitivity will not decrease as rapidly as predicted by equation 2.12. However, since it is difficult to calculate ΔC_{nn}, the magnitude of this decrease on crystal sensitivity cannot be readily estimated.

Part of the apparent increase in crystal sensitivity indicated in Figure 5.2 may also be due to increasing frequency changes caused by crystal heating. Since the data consisted of two sets of films of increasing thickness, the crystal experienced increased heating with each successive film. To correct for this the change in frequency of the monitoring crystal was measured only after the crystal had cooled down as indicated by

a stabilization of its resonating frequency. Provided the
crystal cooled down to its former temperature, then Δf should
be due entirely to the deposited mass on its surface. However,
there are indications that this may take longer than would nor-
mally be expected, and corrections for temperature would have
to be made.

5.6 Frequency Instabilities in the Thickness Monitor

Frequency drifts of the monitor oscillators, together
with frequency changes due to crystal heating are basically the
prime sources of error in a thickness measurement.

In the case of crystal heating two effects occur.
There is a negative transient of several tens of Hz. when the
shutter is opened and positive transient when the shutter is
closed. Figure 5.3 illustrates this behaviour. No material
was deposited on the crystal while the recording was made.
After the initial negative excursion the frequency of the
crystal rises exponentically to a value above its initial fre-
quency. The difference between the initial frequency and the
new equilibrium frequency is due to heating. The positive
excursion behaves similarly. The crystal will stabilize to
its original frequency in time. In Figure 5.3 a part of the
permanent change is probably due to frequency drifts in the
oscillators.

Frequency drifting in the three oscillators, especial-
ly the variable oscillator, is the other prime source of error.
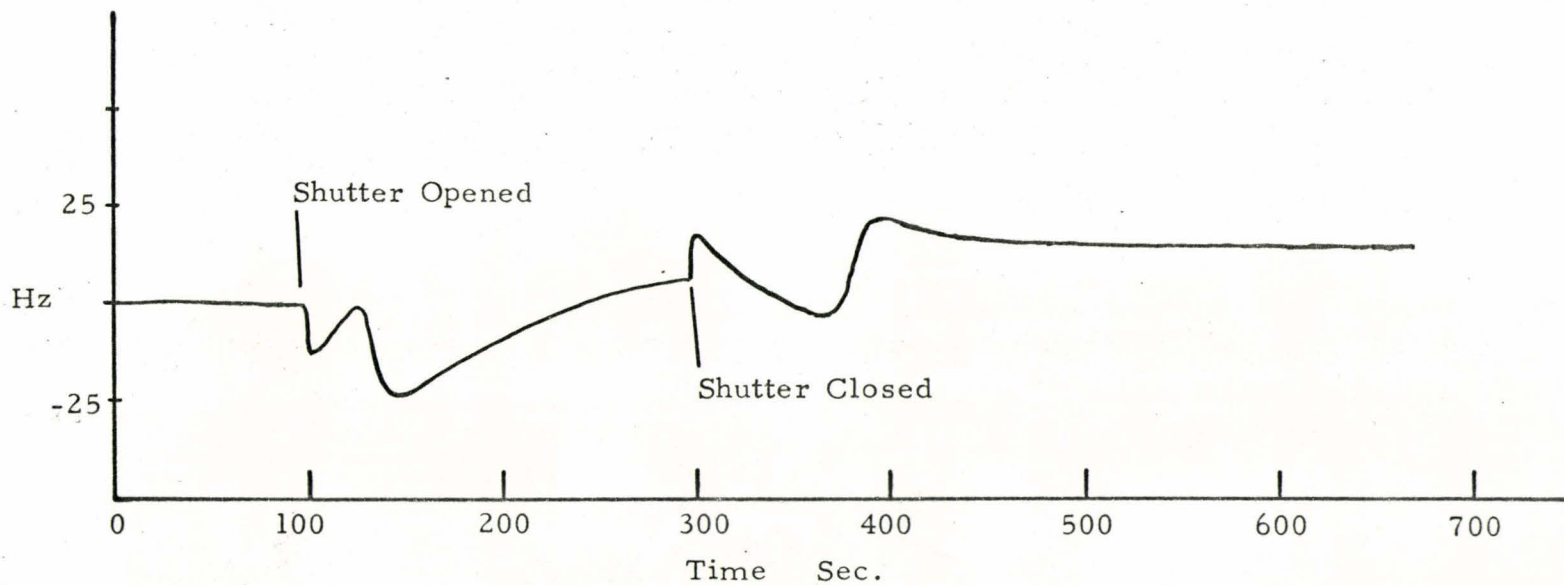
Figure 5.3

Frequency Transients of Monitor Crystal on Opening and
Closing of Source Shutter.

Figure 5.4

Typical Frequency Stability Curves of Thickness Monitor
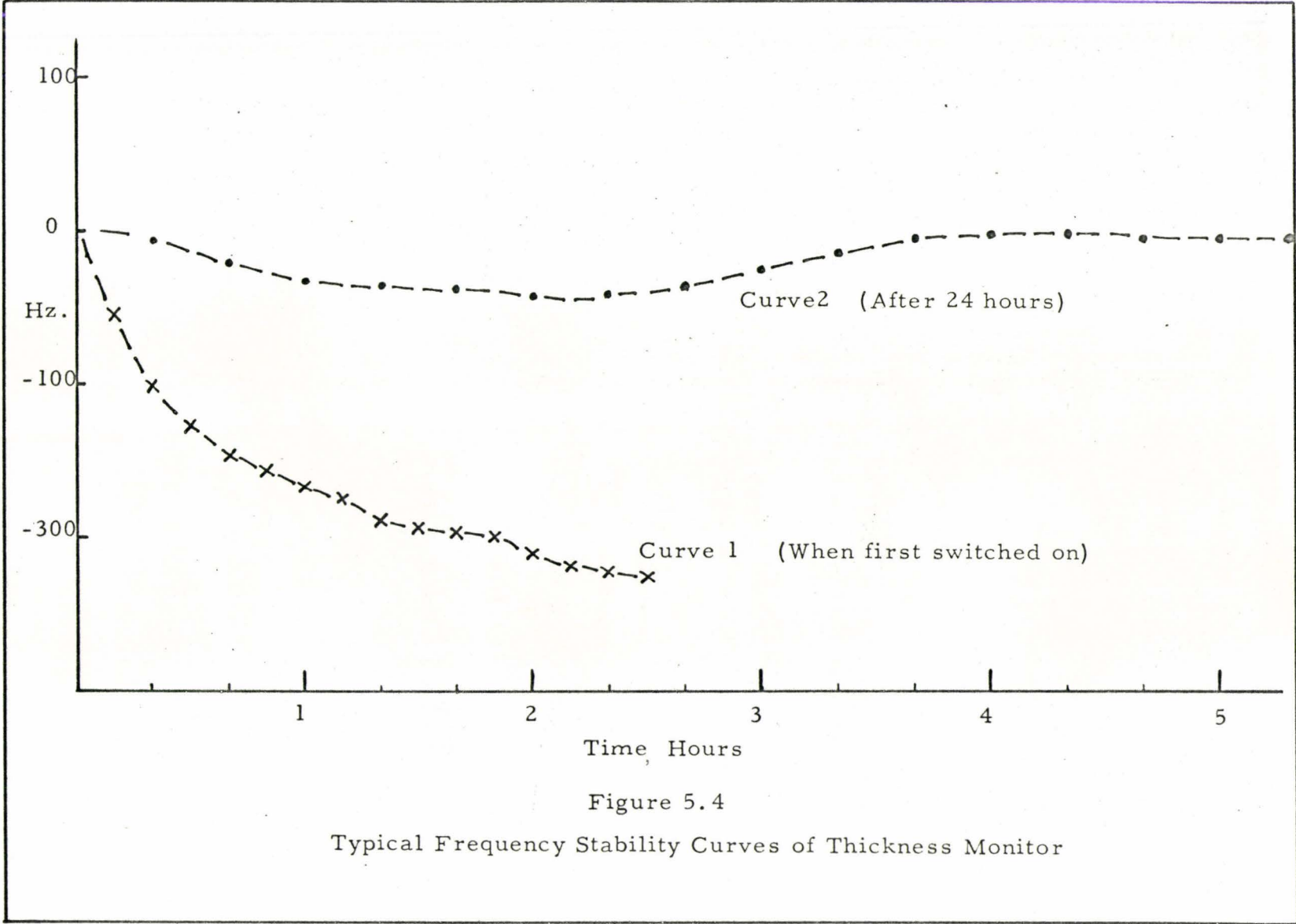
As outlined in chapter three a number of steps were taken to reduce this drift to a minimum. However, it is difficult to avoid this completely without going to elaborate circuit design. In order to determine the overall stability of the oscillator a number of tests were run lasting several hours. The results of two of such tests are shown in Figure 5.4. Curve 1 in Figure 5.4 shows the combined drift in frequency of all three oscillators from the time the monitor was first switched on. Curve 2, on the other hand, shows a similar trace after a 24 hour warm up period.

The monitor was designed primarily for the deposition of thin films. The thickness range of such films extend up to several thousand Angstroms. A typical deposition of such a film may take approximately five minutes. The data in Curve 1 indicates that to get a frequency drift of 10 Hz./5mins. or less, the monitor requires a warm - up period of at least 30 minutes. Curve 2 shows that for longer warm-up periods the frequency drift may go as low as 10 Hz./hour. These drift rates are sufficiently small compared to the frequency change that their effect on Δf may be neglected except perhaps in cases involving relatively thick films and low deposition rates.

5.7 Performance of Controlled Deposition System

The controlled deposition system described in section 3.11 is to be used for preparing thin film passive and active electronic devices. Films deposited for such devices must posses

specific electronic properties e.g. sheet resistance, temperature coefficient of resistance, dielectric coefficient, mobility etc. As indicated at the beginning of this thesis, film thickness and rate of deposition are two of the most critical parameters for controlling film structure and hence, electronic properties. Consequently, the evaluation of the controlled deposition system must be based on how well and how reproducible the system can control thickness and deposition rate.

Constant rate evaporation from a resistance heated source requires that the power input be constant. Most open loop resistance heated sources use a variac type control to adjust the heating current. This is essentially a voltage source and maintains a fixed voltage across the source filament. The current is determined by the resistance of the source. However, during the course of an evaporation the resistance of the source may vary quite widely with resulting changes in source current and hence, power input. Also fluctuations in the supply voltage may occur altering the output voltage of the variac. In either case the change in power input changes the source temperature and hence, the evaporation rate.

Resistance heated sources generally consist of dimpled foil boats of molybdenum or tantalum and tungsten spirals. During a typical evaporation the resistance of these sources is changed because of wetting by the evaporant. Silver or gold, for example, when evaporated from molybdenum has a tendency to

wet the boat. Since they have a much higher conductivity this wetting reduces the boat resistance. If heating is by a voltage source, the current increases and the rate of evaporation goes up with the resultant increase in temperature. This problem is even more aggravated in the case of tungsten spiral sources; here the metal flows along and may wet the entire spiral.

Slag formation on the surface of the evaporant due to impurities may also alter the evaporation rate in that it prevents the evaporant atoms from leaving the surface of the liquid metal. In this case even with a constant current source the evaporation rate cannot be held constant.

The controlled evaporation system outlined in section 3.11 overcomes most of these difficulties because it monitors the rate of evaporation. A feedback loop adjusts the power to the source to compensate for any changes that would tend to alter the evaporation rate from its set value.

To illustrate the degree of rate control possible, a series of four depositon runs were made with silver evaporated from a 5/8 inch wide molybdenum foil boat. The deposition rates chosen were 2, 5, 25 and 50 Hz./sec.; this corresponds to rates of 0.55, 1.35, 6.75 and 13.5 $\overset{\circ}{A}$ /sec. respectively. Traces of the thickness-time plots for these runs are shown in Figures 5.5 and Figures 5.6; they were plotted by chart recorder attached to the film thickness monitor. In each case the slope of the curve gives the deposition rate. From the linearity

End of Deposition

Rate= 1.35 Å/sec.

Rate = 0.55 Å/sec.

27.2 Å
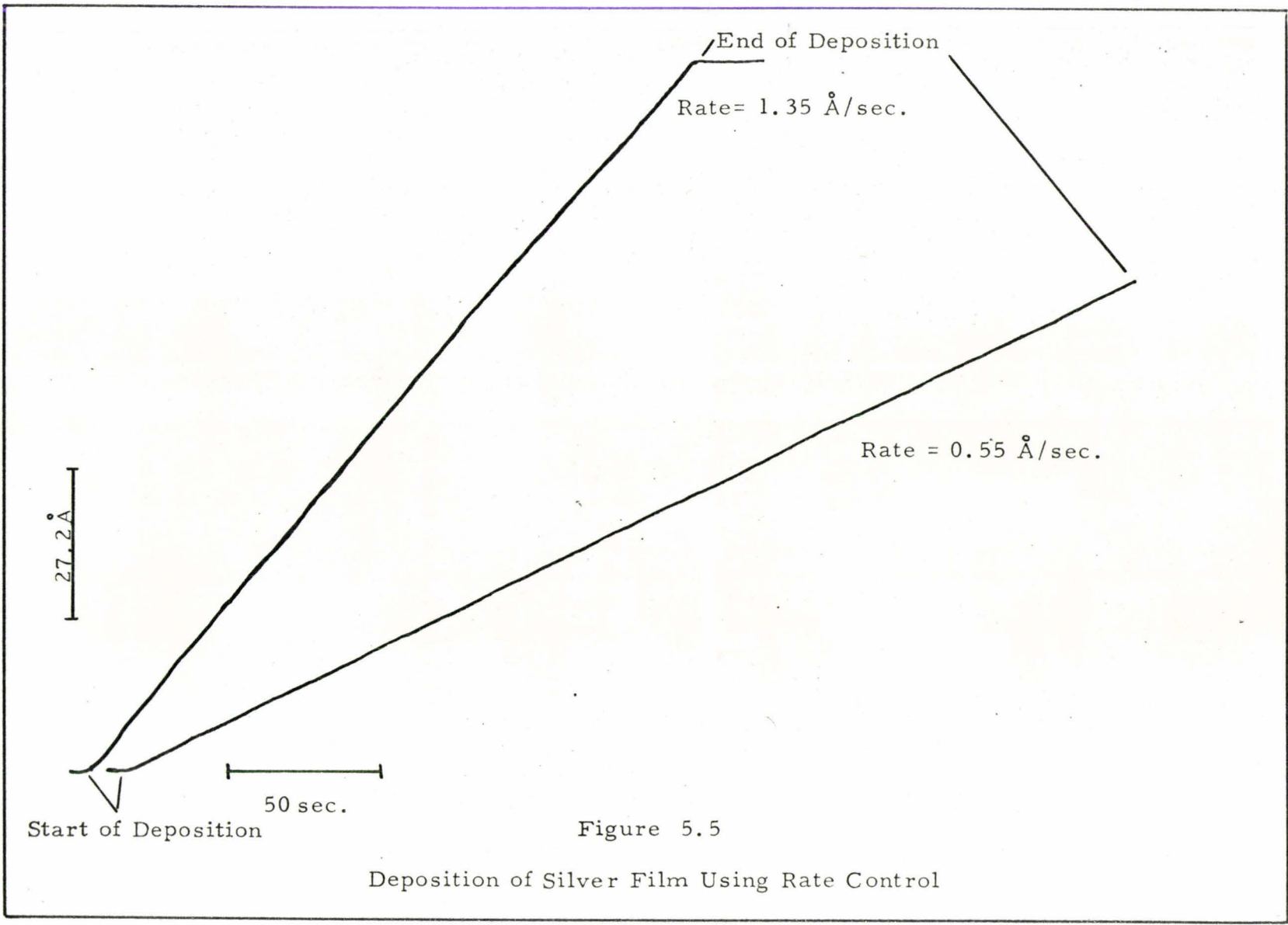
50 sec.

Start of Deposition

Figure 5.5

Deposition of Silver Film Using Rate Control

End of Deposition

Rate =13.5 Å/sec.

Rate = 6.75 Å/Sec.

272 Å

Start of
Deposition

50 Sec.
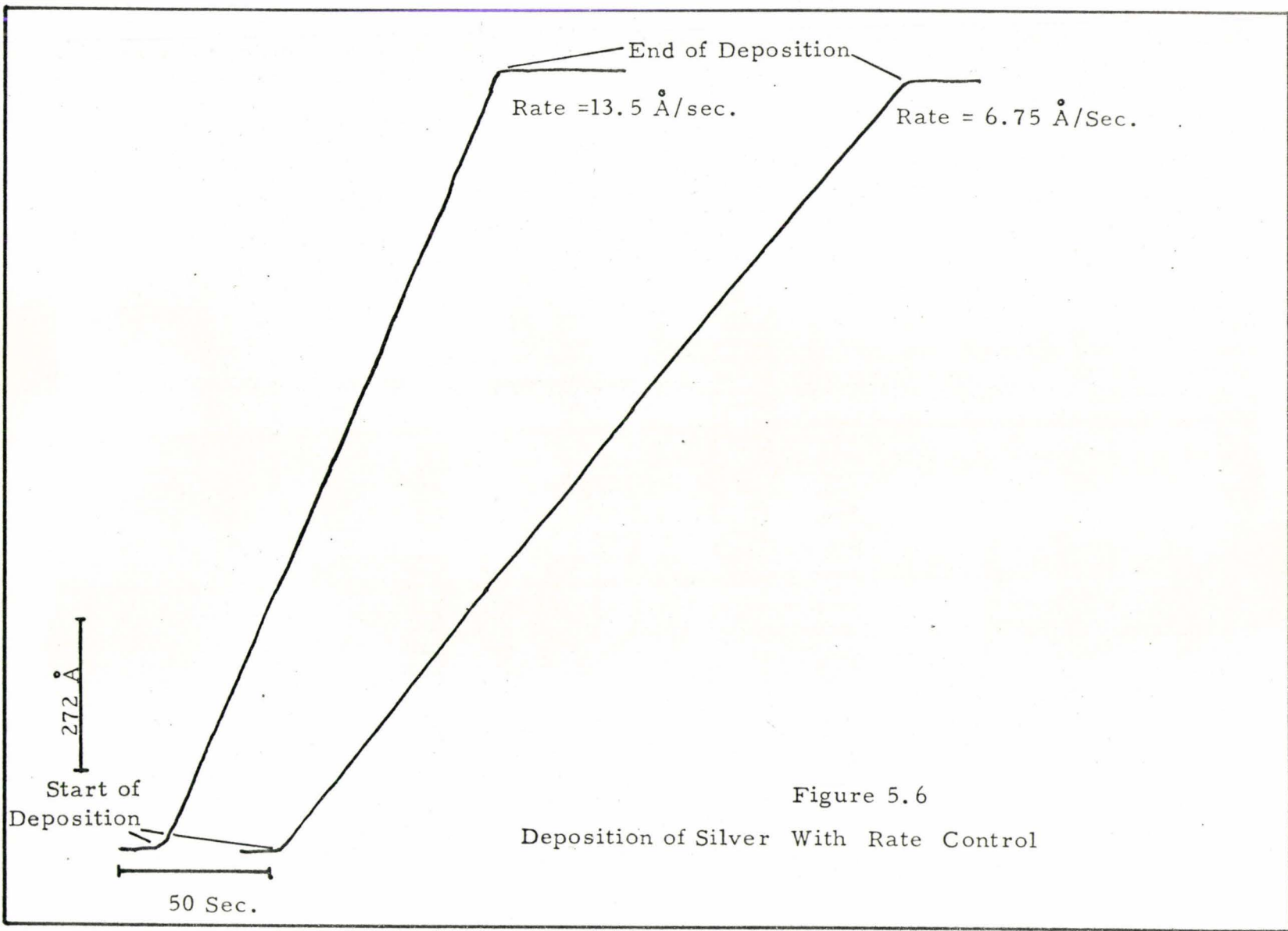
Figure 5.6

Deposition of Silver With Rate Control

of these traces it is evident that excellent rate control can
be obtained with the feedback system. Monitoring the rate of
change of frequency with a digital counter indicated that the
rate varied by less than 5% in each of the traces. This vari-
ation usually occurred in terms of a slow drift spread over
the total deposition time.

In order to compare the evaporation of a system using
rate control with a simple voltage source variac type control,
a series of evaporations were made with various materials e.g.
silver, aluminum, bismuth, SiO and CdS. To discount the fac-
tor of source material depletion affecting depositon rate, all
controlled rate evaporations were made after the evaporations
which were made with variac control. Figure 5.7 shows two
traces of evaporations made with bismuth using variac control
(Curve1) and rate control (Curve2). In Curve 1 the rate varied
anywhere from 0.6 $\mathring{A}$/sec. to 5.5 $\mathring{A}$/sec., while in Curve 2 the
rate remained constant at 4.7 $\mathring{A}$/sec. Bismuth is a particular-
ly sensitive indicator and small current fluctuations cause
relatively large evaporation rates. However, the constant
slope of the Curve 1 indicates that with rate control constant
evaporation rates are assured.

Figure 5.8 shows two evaporations of silicon monoxide,
a dielectric material that can be evaporated from a resistive
heated source. As before Curve 1 is the uncontrolled evapo-
ration and Curve 2 the evaporation with rate control. Again
deposition monitoring and rate control assured constant rate

Curve 2 (With Rate Control)
Rate Constant 4.7 Å/sec

End of Deposition

Curve 1 (Variac Control)
Rate 0.6 -- 5.5 Å/Sec.

End of Deposition

295 Å

Start of Deposition

100 sec

Start of Deposition
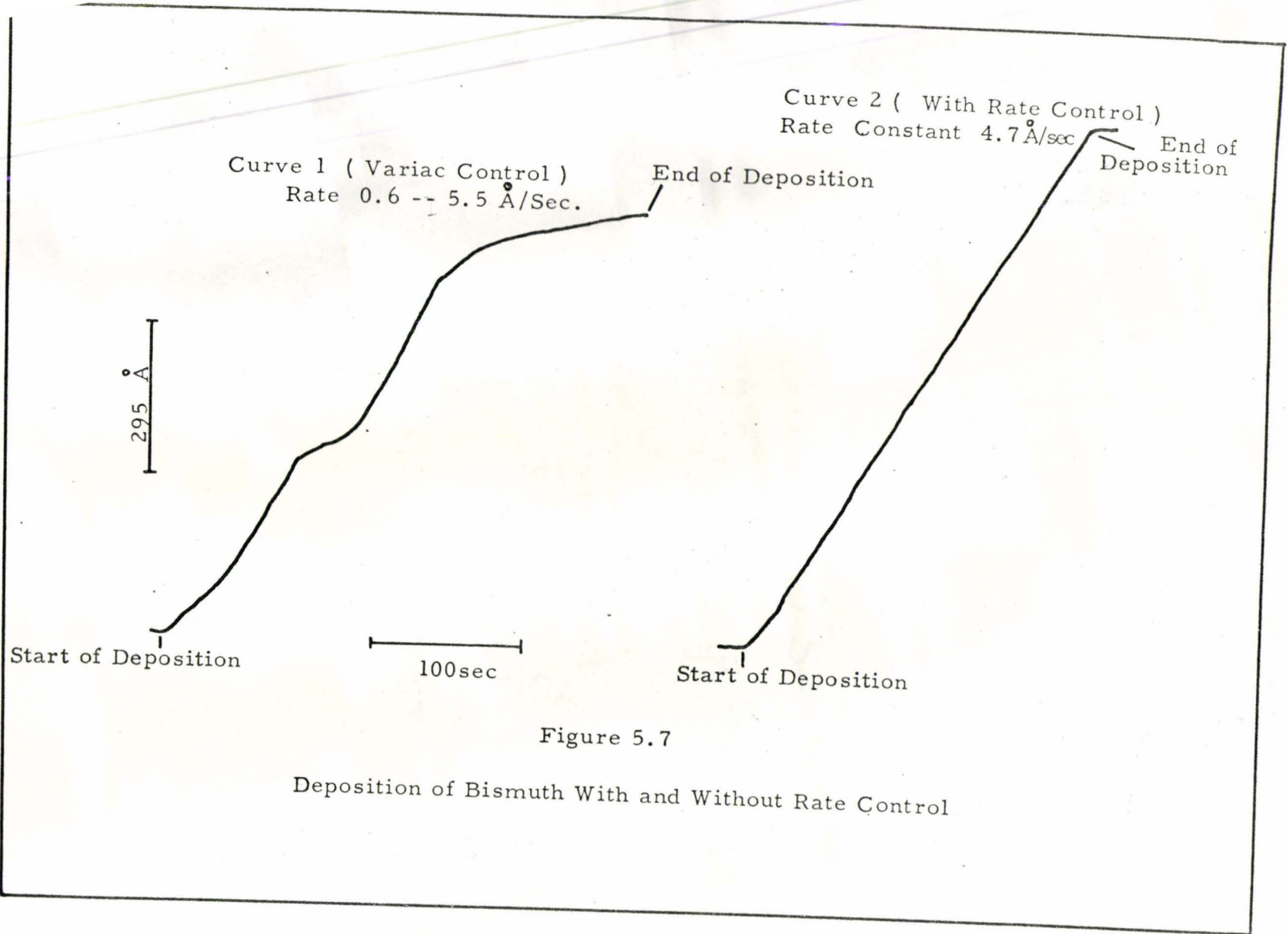
Figure 5.7

Deposition of Bismuth With and Without Rate Control

Curve 1
No Rate Control

End of Deposition

Curve 2
With Rate Control

129 Å

258 Å

100Sec

Start of Deposition

100Sec

Start of Deposition

Figure 5.8

Deposition of SiO With and Without Rate Control
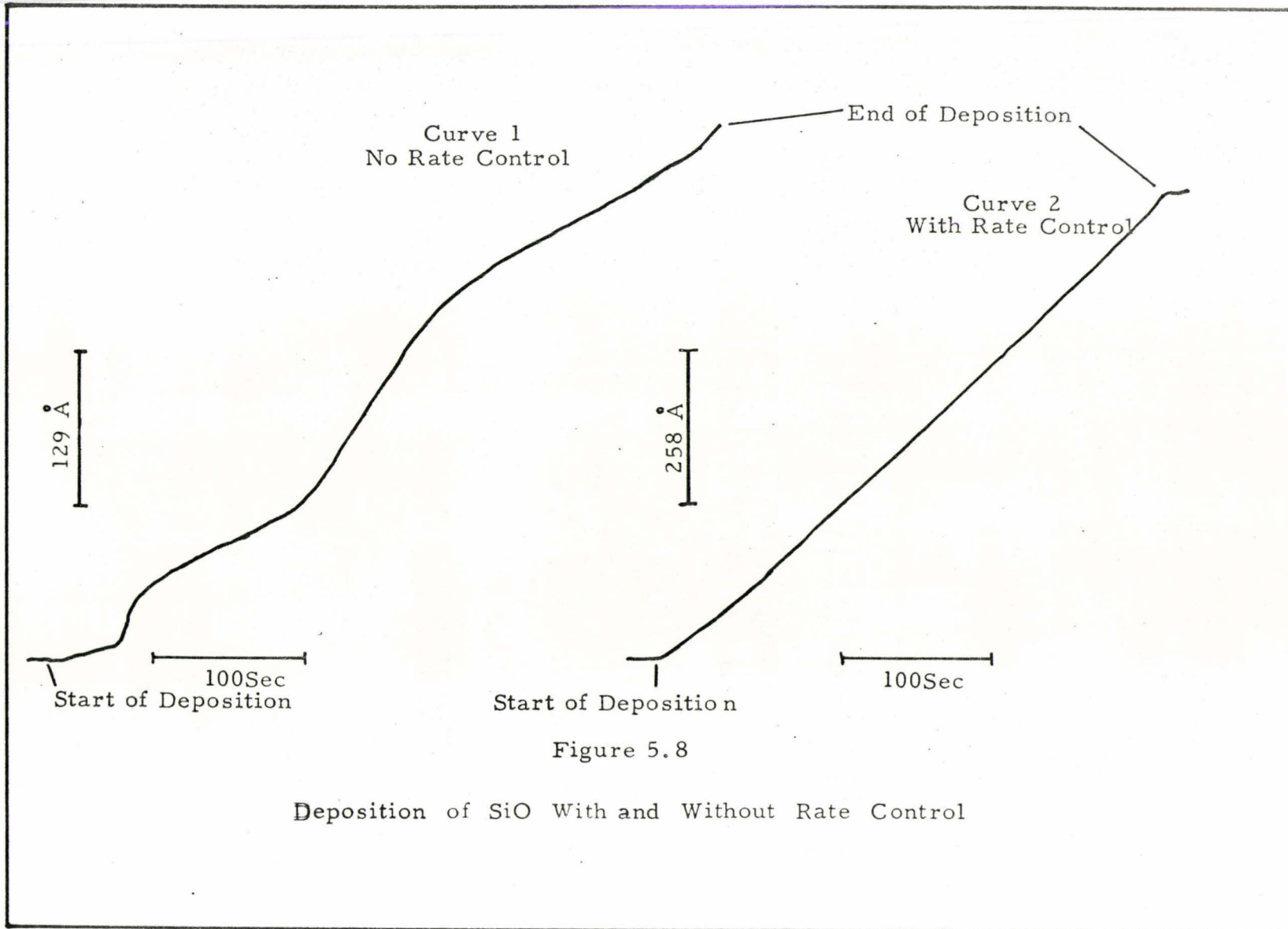
evaporations. Similar control was achieved with cadmium sulphide evaporations. In this case low constant deposition rates are desirable to assure that the stoichiometry of the deposited film is the same as material in the crucible.

One source of frequent evaporation rate changes are fluctuations in the line voltage. A simple variac voltage-source control cannot compensate for fluctuations except by manual readjustment. The advantage of rate control in such a case is shown in Figure 5.9. Curve 1 shows the change in evaporation of a variac controlled source with a -5% deviation in the supply voltage. The rate changed from 1.8 $\overset{o}{A}$/sec. to as low as 0.34 $\overset{o}{A}$/sec. With rate control a similar deviation had little affect on the system the rate staying constant at approximately 2.0 $\overset{o}{A}$/sec.

Curve 1 (Variac Control)

End of Deposition
Curve 2 (Rate Control)

59 Å

Line Voltage Returned to
Normal

Line Voltage down 5%

Start of Deposition

50 Sec

Figure 5.9

Effect of Line Voltage Fluctuation on Evaporation
Rate of Bismuth
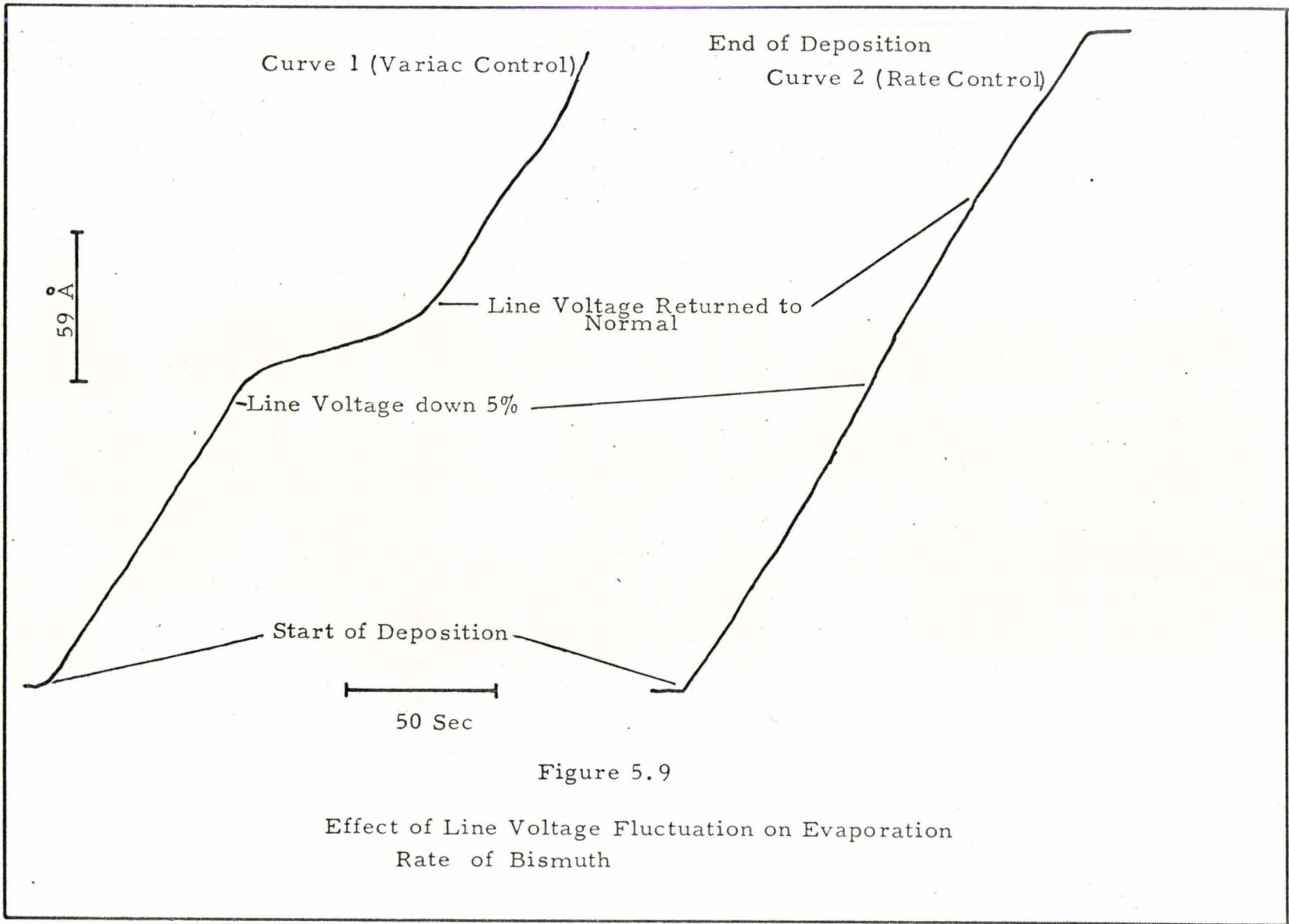
CHAPTER 6

6.1 Conclusions and Recommendations

In this thesis the theory, design and performance of an instrument for measuring and controlling the thickness and deposition rate of thin films evaporated from resistance heated sources has been described and discussed. The principle of operation of this film thickness monitor is based on a resonating quartz crystal sensor. The monitor essentially measures mass in terms of equivalent frequency changes. Hence there may be some doubt about its use when the thin film parameter of interest may be some electrical, optical or other physical property. In practice, however, this is not really a limitation since the changes in frequency may be calibrated in terms of any property that may be of interest.

The quartz crystal monitor offers a number of advantages over other types. Since it is sensitive only to mass, it can be used to monitor the deposition of all types of evaporated material, metals, semiconductors or insulators. Furthermore, it combines the high sensitivity of the quartz crystal with the precision of frequency measurements. Hence the measurement of extremely thin films or low deposition rates can be achieved with relative ease. Finally, the

frequency signals can be converted into analog control signals for controlling the evaporation to achieve constant preset deposition rates.

In the film thickness monitor there are three sources which can introduce errors in the measurement of Δf. These are drifting of the oscillator frequencies, non-linearity in the pulse-analog frequency counter, and heating of the quartz crystal.

In designing the oscillators, steps were taken to stabilize the frequencies. As indicated by the curves in Figure 5.4, the frequency stability may be as low as 10 Hz per hour or less after sufficient warm-up time. Since most typical depositions are of much shorter duration, the effect of frequency drifting can be neglected.

Measurements made on the nonlinearity of the pulse-analog counter, given in Table 2, indicate that even for the simple circuit employed the accuracy over each range is within 2% of full scale deflection and can be increased to 1% by careful calibration. The results from such a simple circuit are due to seperate calibration of each frequency range. The performance of this counter although adequate for the present uses of the monitor, would be improved by employing an operational type integrating circuit.

It is believed that the biggest single source of error in the measurement of Δf is due to heating of the quartz crystal. This problem has no simple solution since the crystal

must be exposed to the radiant heating of the source and the evaporant stream. The zero temperature coefficient of frequency of the Y-cut crystals over the range from -5 to 55°C seems to be inadequate. It was initially felt that frequency changes due to crystal heating could be eliminated by letting the crystal cool to its original temperature. However, this technique, although useful, is aggravated by the frequency transient which occurs when the shutter is closed, and which takes an unknown time to die out.

Although the calibration depositions with silver indicate that the error due to heating is small and can be neglected for most microcircuit depositions, more critical application may require crystal cooling. Alternatively the crystal temperature could be monitored by a thermocouple and corrections made for frequency changes causes by heating.

In designing and aligning the IF and mixer stages some difficulties were experienced with instabilities and bandwidth. The output of the second mixer, for example, requires a bandwidth of 150 KHz and a centre frequency of 575 KHz. It is felt that better performance could be obtained by using RC bandpass networks to achieve the necessary filtering. These can readily be designed with the help of appropriate filter design tables.

The experimental calibration of the monitor crystal with silver was carried out for essentially two reasons. First, the results determined the thickness calibration factor for the

source, crystal and substrate geometry of Figure 5.1. It is important to realize that this calibration is applicable only to a small area directed surface evaporation source together with the above configuration. If any of the dimensions are changed including the source then the system must be recalibrated.

Secondly, the depositions indicate that within the experimental error the theoretical "mass determination sensitivity", C_f, was essentially realized. This means that for the particular quartz crystals used, the active, resonating area is equal to or less than 0.635 cm (0.25 in.) in diameter. This is an important result, since it means that the thickness calibration factor could have been calculated from a knowledge of the system geometry without a long and tedious experimental calibration. Furthermore changes in the evaporation source and system geometry can be made to optimize a particular deposition and the new calibration factors readily calculated.

In the introduction to this thesis it was indicated that the rate of deposition and film thickness are two of the most critical parameters for determining the properties of a vacuum evaporated film. Furthermore, in the evaporation of certain films rate control is essential. The evaporation of CdS for thin film active devices, for example, requires deposition rates of 1 Å/sec. or less to avoid getting cadmium enriched films. The evaporations made with Ag, Bi, SiO, CdS

etc., some of which are shown in section 5.7, indicate that the quartz crystal monitor together with the controlled evaporation system described in section 3.11 can indeed achieve these low constant evaporation rates.

It is felt that a controlled rate evaporation system is an essential requirement for any serious investigation of in vacuo deposited films for thin film micro-circuit application or otherwise. It permits, for example, investigations of reactive evaporation, where the growth of a chemical compound is controlled by evaporating at constant rates in a gas atmosphere. Moreover, by including another monitor in the system to control a second evaporation source, compounds can be prepared without the use of flash evaporation techniques. The apparatus assembled for the present work is to be used for investigations in some of these areas.

APPENDIX 1

List of Component Values of Thickness Monitor
of Figures 3a and 3b

Resistors Ohms

R1	47K	R32	10K	R63	10K
R2	56K	R33	3K Pot.	R64	25K Pot.
R3	4.7K	R34	560	R65	25K Pot.
R4	33K	R35	33K	R66	25K Pot.
R5	47K	R36	4.7K	R67	25K Pot.
R6	10K	R37	1K	R68	10K
R7	470	R38	470	R69	10K Pot.
R8	50	R39	2.2K	R70	4.7K
R9	47K	R40	2.2K	R71	4.7K
R10	56K	R41	1K	R72	10K
R11	10K	R42	2.7K	R73a	10
R12	1K	R43	7.8K	R73b	5K Pot.
R13	2.2K	R44	3.3K	R74a	1.0M
R14	56K	R45	1.0K	R74b	10K
R15	4.7K	R46	470	R75	2.2K
R16	470	R47	10K Pot.	R76	50K Pot.
R17	2.2K	R48	270	R77	5K Pot.
R18	47K	R49	270	R78	220
R19	56K	R50	220	R79	50K Pot.
R20	56K	R51	4.7K	R80	22M
R21	56K	R52	1.5K	R81	10K
R22	2.2K	R53	2.2K	R82	10K
R23	2.2K	R54	3.3K	R83	34K
R24	6.8K	R55	3.3K	R84	750K
R25	2.2K	R56	6.8K	R85	2.2K
R26	1.8K	R57	15K	R86	1K Pot.
R27	100	R58	8.2K	R87	2.2K
R28	3.3K	R59	1.0K	R88	10K
R29	15K	R60	10K	R89	2.2K
R30	30K	R61	100K	R90	490
R31	29K	R62	1.0K	R91	100K

Capacitors

All Values in Microfarads Unless Noted Otherwise

C1	100	pf.	C20	10	pf.	C39	.05	
C2	430	pf.	C21	68	pf.	C40	220	
C3	.01		C22	10	pf.	C41	0.1	
C4	.001		C23	320	pf.	C42	.01	
C5	.01		C24	.05		C43	.001	
C6	50		C25	.005		C44	220	pf.
C7	.01		C26	50	pf.	C45	.01	
C8	.01		C27	0-300pf.		C46	.002	
C9	.022		C28	0-20 pf.		C47	.001	
C10	.01		C29	.01		C48	220	pf.
C11	.001		C30	.01		C49	50	
C12	100	pf.	C31	.01		C50	.001	
C13	.022		C32	10		C51	10.0	
C14	680	pf.	C33	1530	pf.	C52	0.1	
C15	50		C34	1750	pf.	C53	.05	
C16	100		C35	1280	pf.	C54	1000	
C17	10		C36	800		C55	100	
C18	50		C37	100		C56	100	
C19	0.1		C38	10		C57	500	
						C58	500	

Inductances

L1	14.8 - 31 micro H.	L4	1.08 mH
L2	14.8 - 31 micro H.	L5	2.08 mH
L3	14.8 - 31 micro H.	L6	2.07 mH

TR 1, TR 2, Modified 4.7 MHz IF Transformer
TR 3   Modified 455 KHz IF Transformer

TR 4,   115 V. A.C. Primary Power, Transformer
         36 V Secondary

SW1   Double Pole-4 Position, Two Deck Rotary Switch
SW2   Double Pole-3 Position, Single Deck Rotary Switch
SW3   DPST On-Off Toggle Switch

M_1 DC Milliammeter 1mA f.s.d., 100 divisions

M_2 DC Microammeter 100 micro A f.s.d., 100 divisions

Transistors

All Transistors NPN Silicon (G. E. Plastic Coated)

2N3860	T1
2N3859	T6, T12
2N3856A	T4, T5, T7, T8, T9
2N3854A	T2, T3
2N3605	T16, T17, T18, T19
2N3414	T20, T21
2N3393	T22, T23
2N3392	T15
2N2924	T10, T11, T13, T14
TR02C PNP Power	T24

Diodes

D1   IN4009
D2, D3 1601   G.E. Dual Diode
D4, D5 IN 482
D6, D7, D8, D9   IN2070 Rect. 0.5 Amps P.I.V. 400 Volts

Z1   IN961 10 Volts
Z2   OAZ204 6.8 Volts
Z3   IN965B 15 Volts

REFERENCES

1. Holland, L., _Vacuum Deposition of Thin Film_,
    John Wiley & Sons Inc., New York, 1961, p. 199-232.

2. Hass, G., Thun, R. Ed. _Physics of Thin Films_ Vol. 3,
    Academic Press, New York, 1966, p. 211-219.

3. Tolansky, S., _Multiple Beam Interferometry of Surfaces
    and Films_, Oxford University Press, Oxford, 1948.

4. Stechelmacher, W., English, J., " Instrument for the
    controlled Deposition of Optical Film Systems", Trans.
    8th Nat. Vac. Symp., Pergamon Press, Oxford, 1962.

5. Hayes, R. E., Roberts, A. R. V., " A Control System for
    the Evaporation of Silicon Monoxide Insulating Films",
    J. Sci. Instruments 39, p. 428.

6. Haase, O., " On the Measurement with an Ionization Guage
    of the Density of a Vapour Stream for the Production of
    Thin Films on a Substrate", Z. der Naturforschung 12a
    No. 11, p. 941.

7. Giedd, G. R., Perkins, M. H., " Evaporation Rate Monitor",
    Rev. Sci. Instruments, 31, p. 773.

8. Sauerbrey, G., " Verwendung von Schwingquarzen zur
    Waegung duenner Schichten und zur Mikrowaegung",
    Zeitschriften der Physick 155, p. 206-222. (1959)

9. Warner, A. W., Stockbridge, C. D., "Mass and Thermal
    Measurement with Resonating Crystalline Quartz",
    Vacuum Microbalance Techniques, Vol. 2, Plenum Press
    New York, 1962, p. 71-92.

10. Haller, J., White, P., " Simple High Sensitive Micro-
    balance for use in U.H.V.", Rev. Sci. Instruments, 34,
    June, 1963, P. 677.

11. Wade, W. H, and Slutsky, L. J., " Adsorption on Quartz
    Single Crystals", Vacuum Microbalance Techniques Vol. 2,
    Plenum Press New York, 1962.

12. Mason, W. P., _Piezoelectric Crystals and their Application
    to Ultrasonics_, D. Van Nostrand Co., Inc., New York, 1950.

13. Willard, G. W., and Hight, S. C., Proc. IRE Vol. 25
    p. 549-563.

14. Stockbridge, C.D., "Resonance Frequency Versus Mass
    added to Quartz Crystal", Vacuum Microbalance Tech-
    niques, Vol. 5, Plenum Press, New York, 1966, p. 193.

15. Strutt, J. W., (Lord Rayleigh), The Theory of Sound,
    rev. ed. Dover Publications, New York, 1945, p. 113-118.

16. Lawson, W. H., " A versatile Thin Film Monitor of High
    accuracy", J. Sci. Instruments, Vol. 44, 1967, p. 917.

17. Stockbridge, C. D., Warner, A. W., " A Vacuum System for
    Mass and Thermal Measurement with Resonating Crystalline
    Quartz", Vacuum Microbalance Techniques, Vol. 2, Plenum
    Press, New York, 1962, p. 93.

18. Warner, A. W., Stockbridge, C. D.,Journal of Applied
    Physics, Vol. 34, p. 437, 1963.

19. Behrndt, K. H., Physics of Thin Films, Vol. 3, Hass, G.,
    Thun, R., Ed., Academic Press, London, 1966, p. 23.

20. Knudsen, M., The Kinetic Theory of Gases Methuen & Co.
    Ltd., (London), 1934, p. 26.

21. Holland, L., Vacuum Deposition of Thin Films, John Wiley &
    Sons Inc., New York, 1961, p. 158, p. 166-167.

22. Holland, L., opus cit, p. 145-146.

23. Steckelmacher, W., Thin Film Microelectronics,
    L. Holland, Ed., Chapman and Hall Ltd., Lond, 1965, p. 215.

24. Steckelmacher, W., opus cit. p. 213.

25. Reich, H. J., Functional Circuits and Oscillators
    D. Van Nostrand Co. Inc., Princeton New Jersey, 1962.

26. Hunter, L. P., Ed., Handbook of Semiconductor Electronics
    The MacMillan Company, New York, 1964.

27. Walston, J. A., Miller, J. R., Ed., Transistor Circuit
    Design, McGraw Hill Book Co., Inc., New York, 1963.

28. Clapp, J. K., Proc. IRE, Vol. 36, March 1958, p. 356-358.

29. Roberts, W. A., Proc. IRE, Vol 36, Oct. 1948, p. 1126-1262.

30. Sturley, K. R., Ed., Radio Receiver Design, 3rd. Ed.,
    Chapman & Hall, London, 1965, p. 456.

31. Weinberg, l., Network Analysis and Synthesis, McGraw Hill
    Book Co. Inc., New York, 1962.

32. Philbrick Applications Manual, Philbrick Researches Inc.
    p.49.

33. Turner, J. A., Birtwistle, J. K., and Hoffman, G. R.,
    " A Method for continuous Measurement of Thickness and
    Deposition Rate of Conduction Films during Vacuum
    Evaporation", J. Sci. Instruments 40, p. 557.

34. Steckelmacher, W., Thin Film Microelectronics, Holland, L.,
    Ed., Chapman and Hall, London, 1965, p. 231-239.

35. Bath, H. H. A., English, J., and Steckelmacher, W.,
    "Automatic Control and Monitoring System for Thin Film
    Deposition", Electronic Components, March 1966, p. 239-247.

36. Bath, H. H. A., Steckelmacher, W., "Vacuum Evaporation Rate
    Control by use of Constant Source Current", J. Sci. Instru-
    ments, 42, p. 144-146.

37. Holland, L., Vacuum Deposition of Thin Films, John Wiley &
    Sons, New York, 1961, p. 224, p. 231.